Journal Pre-proof

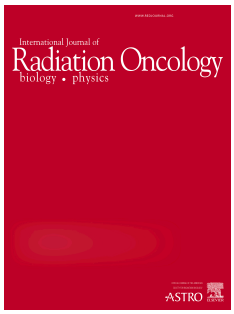

Accounting for range uncertainties in the optimization of combined proton-photon treatments via stochastic optimization

Mark Bangert, PhD, Matthias Guckenberger, MD, Jan Unkelbach, PhD, Silvia Fabiano, MSc

PII: S0360-3016(20)31055-5

DOI: https://doi.org/10.1016/j.ijrobp.2020.04.029

Reference: ROB 26316

To appear in: *International Journal of Radiation Oncology • Biology • Physics*

Received Date: 29 November 2019

Revised Date: 16 March 2020

Accepted Date: 20 April 2020

Please cite this article as: Bangert M, Guckenberger M, Unkelbach J, Fabiano S, Accounting for range uncertainties in the optimization of combined proton-photon treatments via stochastic optimization, *International Journal of Radiation Oncology • Biology • Physics* (2020), doi: https://doi.org/10.1016/j.ijrobp.2020.04.029.

Manuscript title

Accounting for range uncertainties in the optimization of combined proton-photon treatments via stochastic optimization

Short running title

Robust combined proton-photon treatments

First author and corresponding author:

Silvia Fabiano, MSc

Department of Radiation Oncology, University Hospital Zürich

Mail: Rämistrasse 100, 8091 Zürich, Switzerland

Email: silvia.fabiano@usz.ch

Phone: +41 44 255 21 83

Coauthors:

Mark Bangert, PhD

Department of Medical Physics in Radiation Oncology, German Cancer Research Center, Heidelberg, Germany

Matthias Guckenberger, MD

Department of Radiation Oncology, University Hospital Zürich, Switzerland

Senior author:

Jan Unkelbach, PhD

Department of Radiation Oncology, University Hospital Zürich, Switzerland

Conflict of interest: none

Funding statement: This research did not receive any specific grant from funding agencies in the public, commercial, or not-for-profit sectors.

Acknowledgments: none

Abstract

Purpose: Proton treatment slots are still a limited resource. Combined proton-photon treatments, in which most fractions are delivered with photons and only a few with protons, may represent a practical solution to optimize the allocation of proton resources over the patient population. We demonstrate how a limited number of proton fractions can be optimally used in multi-modality treatments, also addressing the issue of the robustness of combined treatments against proton range uncertainties.

Materials and Methods: Combined proton-photon treatments are planned by simultaneously optimizing intensity-modulated radiation therapy (IMRT) and proton therapy (IMPT) plans while accounting for the fractionation effect through the biologically effective dose (BED) model. The method is investigated for different tumor sites (a spinal metastasis, a sacral chordoma, and an atypical meningioma) in which organs at risk (OARs) are located within or near the tumor. Stochastic optimization is applied to mitigate range uncertainties.

Results: In optimal combinations, proton and photon fractions deliver similar doses to OARs overlaying the target volume to protect these dose-limiting normal tissues through fractionation. Meanwhile, parts of the tumor are hypofractionated with protons. Thus, the total dose delivered with photons is reduced compared to simple combinations where each modality delivers the prescribed dose per fraction to the target volume. The benefit of optimal combinations persists when range errors are accounted for via stochastic optimization.

Conclusions: Limited proton resources are optimally used in combined treatments if parts of the tumor are hypofractionated with protons while near-uniform fractionation is maintained in serial OARs. Proton range uncertainties can be efficiently accounted for through stochastic optimization and are not an obstacle for clinical application.

1. Introduction

Recently, there has been growing interest in proton therapy mainly owing to the unique depth-dose curve characteristics of protons compared to photons. Although the number of proton therapy centers has increased worldwide over the past decades, to date proton treatment slots are still a limited resource [1].

Currently, different countries develop guidelines to decide which patients are eligible for proton therapy [2-4]. To maximize the benefit of proton therapy for the entire patient population, combined proton-photon treatments, in which most fractions are delivered with photons and only a few with protons, might play a role [5-8]. In that context, the question arises how a limited number of proton fractions can be optimally used in multi-modality treatments. Institutions performing combined treatments optimize IMRT and IMPT plans separately so that each modality delivers the prescribed dose per fraction to the target volume [9]. Recently, several authors have investigated approaches to improve on such simple proton-photon combinations. Ten Eikelder *et al* [7] still consider separately planned proton and photon treatment plans, however, the dose per fraction delivered with protons and photons may be different and is optimized using BED criteria. Gao [10] simultaneously optimize IMRT and IMPT plans based on their cumulative physical dose, however, additional objectives are introduced to enforce that both modalities individually deliver homogeneous doses to the target volume. XXX [8] developed a method to simultaneously optimize IMRT and IMPT plans based on BED to account for the fractionation effect. Optimized proton-photon combinations were investigated for tumor sites where serial OARs are located within or near the tumor. In this case, proton and photon fractions must deliver similar doses to the OARs overlaying the target volume to protect these dose-limiting normal tissues through fractionation. Meanwhile, if parts of the target volume are hypofractionated with protons, the

total dose delivered with photons can be reduced, leading to a reduction of the integral dose to normal tissues.

As a next step towards the implementation of optimized proton-photon therapy, one needs to address the robustness of such non-trivial combined treatments with respect to delivery uncertainties. The dose distribution delivered to the patient may highly degrade compared to the planned one if these errors are not accounted for during treatment planning. In radiotherapy, uncertainties are typically handled by using safety margins. Recently, robust planning methods that directly include uncertainties in treatment plan optimization have been developed [11-17].

In this work, we further investigate the benefit of jointly optimized proton-photon treatments, also addressing the issue of the robustness of non-trivial combined treatment plans against proton range uncertainties. We apply a stochastic optimization technique [11] that directly incorporates proton range uncertainties into the multi-modality treatment plan optimization problem. We focus only on range uncertainties while accounting for other potential sources of errors through safety margins [18]. The approach is applied to a spinal metastasis, a sacral chordoma, and an atypical meningioma, to demonstrate the method for a variety of potential clinical applications.

2. Materials and methods

2.1. Mathematical model of the fractionation effect

Optimal combined proton-photon treatments must account for the fractionation effect. The most widely used model to mathematically describe the fractionation effect is the BED model [19]. For this work, we consider a generalization of the standard BED model to multi-modality treatments. We assume that the model can be extended to fractionation schemes in which

protons and photons deliver different doses per fraction. Therefore, the cumulative BED b over an entire combined proton-photon treatment with n^{γ} photon fractions and n^{p} proton fractions is given by:

$$b = n^{\gamma} d^{\gamma} \left(1 + \frac{d^{\gamma}}{\alpha/\beta}\right) + n^{p} d^{p} \left(1 + \frac{d^{p}}{\alpha/\beta}\right) \quad (1)$$

where d^{γ} and d^{p} are the physical doses per fraction for photons and protons, respectively, and the α/β-ratio is a tissue-specific parameter. In accordance with current clinical practice, the proton dose per fraction d^{p} includes a constant relative biological effectiveness (RBE) factor of 1.1, which we do not make explicit in Eq. 1.

For visualization and quantitative interpretation, the BED distribution can be scaled as shown in Eq. 2. This corresponds to the definition of the equieffective dose ($EQDX$) that can be interpreted as the total physical dose that needs to be delivered in a uniformly fractionated treatment with a dose per fraction of X Gy to achieve the same BED b.

$$EQDX = \frac{b}{\left(1 + \frac{X}{\alpha/\beta}\right)} \quad (2)$$

2.2. Multi-modality treatment plan optimization

Combined proton-photon treatments are obtained by simultaneously optimizing IMRT and IMPT plans using the concept of cumulative BED b according to Eq. 1. Planning is performed using an in-house developed research software. Range uncertainties are modeled via three scenarios: the nominal scenario, the overshoot and undershoot scenarios. The stochastic programming approach is used to incorporate the set of error scenarios into the planning of combined treatments. The method minimizes a weighted sum of objective functions f for BED

evaluated for all error scenarios. Formally, the optimization problem is:

$$\underset{x^\gamma, x^p}{\text{minimize}} \quad \sum_s p_s f(\boldsymbol{b}^s) \tag{3}$$

$$\text{subject to} \quad c_m(\boldsymbol{b}^s) \leq u_m \qquad \forall m, s \tag{4}$$

$$b_i^s = n^\gamma d_i^\gamma \left[1 + \frac{d_i^\gamma}{(\alpha/\beta)_i}\right] + n^p (d_i^p)^s \left[1 + \frac{(d_i^p)^s}{(\alpha/\beta)_i}\right] \qquad \forall i, s \tag{5}$$

$$d_i^\gamma = \sum_j D_{ij}^\gamma x_j^\gamma \qquad \forall i \tag{6}$$

$$(d_i^p)^s = \sum_k (D_{ik}^p)^s x_k^p \qquad \forall i, s \tag{7}$$

$$x_j^\gamma \geq 0 \qquad \forall j \tag{8}$$

$$x_k^p \geq 0 \qquad \forall k \tag{9}$$

where u_m are upper bounds for the constraint functions $c_m(\boldsymbol{b}^s)$, x_j^γ and x_k^p are the intensities of beamlet j and pencil beam k in the IMRT and IMPT plans, and the dose-influence matrix elements D_{ij}^γ and D_{ik}^p denote the dose contributions of beamlet j and pencil beam k to voxel i for unit intensity. The parameter p_s represents an importance weight for error scenario s. Typically, a higher weight is given to scenarios that are more likely to occur.

2.3. Clinical cases

We investigated the benefit of jointly optimized proton-photon combinations for the three clinical cases shown in Figure 1.

2.3.1. Spinal metastasis case

The spinal tumor entirely surrounds the cauda (Figure 1a). A 3 mm expansion of the cauda to a planning risk volume (PRV) is considered to ensure the sparing of this serial structure

despite setup errors and contouring uncertainties.

Treatment planning aims at delivering a BED_{10} corresponding to a dose of 35.2 Gy in 5 fractions to the planning target volume (PTV). The maximum BED_2 in the cauda and PRV is constrained to 60 Gy and 112 Gy, respectively, corresponding to a dose of 20 and 28.8 Gy in 5 fractions. Additional planning objectives are conformity as well as minimizing the mean BED_2 in the normal tissues surrounding the tumor (further details are provided in Appendix A and Table A.1a).

2.3.2. Sacral chordoma case

For the sacral chordoma case, the gross tumor volume (GTV) borders bowel, rectum, and bladder (Figure 1b). The clinical target volume (CTV) is a 0-15 mm expansion of the GTV to encompass microscopic diseases. To account for setup errors, a 5 mm expansion of CTV-to-PTV is considered. Treatment planning aims at delivering a BED_{10} equivalent to a dose of 70 Gy and 54 Gy in 30 fractions to the GTV and PTV, respectively. Additional objectives are used to achieve conformity and to minimize the mean BED_4 in the healthy tissues. The mean BED_4 in the OARs (bowel, rectum, and bladder) is minimized while the maximum dose is constrained to the BED_4-equivalent of 54 Gy in 30 fractions (see Table A.1b, Appendix A).

2.3.3. Atypical meningioma

For the atypical meningioma case, the PTV overlays the brainstem, optic nerves and pituitary gland (Figure 1c). Treatment planning aims at delivering a BED_{10}-equivalent to a dose of 54 Gy in 30 fractions to the GTV and PTV. Additional objective functions represent the goals of conformity, minimization of the generalized equivalent uniform dose (gEUD) in

the brainstem and minimization of the mean BED_2 in the normal brain. The maximum BED_2 in the OARs is constrained to 102.6 Gy, corresponding to a physical dose of 54 Gy in 30 fractions. Plan and dose parameters are listed in Table A.1c (Appendix A).

2.4. Assessing the benefit of optimized combined treatment

Differences between optimized proton-photon treatments and simple combinations of IMRT and IMPT plans are quantified according to the following procedure. We first optimize single-modality IMRT and IMPT plans based on the same set of objective and constraint functions. The IMRT plans consist of 19-equispaced coplanar beams. The IMPT plan uses 2-3 fields depending on the case. We then generate a *reference plan* as a simple proportional combination of the single-modality plans. Finally, we obtain a combined proton-photon plan by optimizing a subset of the objectives (namely the mean BED in OARs and healthy tissues surrounding the tumor) while constraining all the remaining objective functions to be no worse than their values in the reference plan. Initially, we do not account for range uncertainties in treatment planning optimization. We then apply probabilistic planning to make treatment plans more robust against range errors. To that end, we set $p_1 = 0.5$ for the nominal scenario and $p_2 = p_3 = 0.25$ for the undershoot and overshoot scenarios [13, 20]. As a conservative estimate, range errors are modeled by uniformly scaling the CT Hounsfield units by ±5%. Further details of treatment plan optimization can be found in Appendix A.

3. Results

3.1. Spinal metastasis case

Figures 2a and 2b show the non-robust single-modality IMRT and IMPT plans, each delivering 7 Gy per fraction to the PTV. Figure 2c shows the cumulative equieffective dose EQD7.04 for the

non-robust reference plan, which uses 1 IMPT and 4 IMRT fractions. For comparison, Figures 2d and 2e show the IMRT and IMPT dose distributions in the non-robust optimized combination. Protons and photons deliver similar doses per fraction to the PRV. However, a photon fraction delivers a mean dose of 3.7 Gy to the target volume, while a proton fraction delivers a mean dose of 15.4 Gy (see also Figure B.1a, Appendix B). Figure 2f shows the cumulative equieffective dose EQD7.04 for the non-robust optimized combination. Protons and photons together yield a conformal treatment plan that delivers the prescribed BED to the target volume. However, as less dose is delivered with photons, the optimized combination achieves 91% of mean BED reduction in normal tissues that a 5-fraction IMPT plan yields, compared to 20% for the reference plan.

Figures 3a-c show the results of a sensitivity analysis to range errors for the non-robust plans. All the plans yield similar target coverage and a good sparing of the spinal cord for the nominal scenario (Figure 3a). However, range errors may highly degrade the dose distribution causing hot and cold dose spots within the target volume as well as undesired high doses to the cauda (Figures 3b-3c). The dose degradation is less severe for the reference plan than for the single-modality IMPT plan and the optimized combination. This is due to the fact that the reference plan uses 4 IMRT and 1 IMPT fractions each delivering the same dose per fraction to the target volume. However, the IMRT fractions do not degrade. In contrast, the dose distribution for the optimized combination is highly degraded as most of the prescribed BED to the target is delivered in a single IMPT fraction.

Accounting for range uncertainties via stochastic optimization leads to the robust plans shown in Figures 2g-i and 2l-n for the nominal scenario. Figure 2i shows the robust reference plan which consists of one robustly optimized IMPT fraction (Figure 2h), and 4 IMRT fractions (Figure 2g) that are identical to Figure 2a. In the robustly optimized combination (Figures 2l-n),

the photon fractions (Figure 2l) deliver on average higher doses to the parts of the target volume adjacent to the cauda compared to the non-robust combination (Figure 2d), while the proton fraction hypofractionates the peripheral parts (Figure 2m and Figure B.1b). Consequently, the robustly optimized combination achieves 54% of the mean BED reduction in normal tissues that is possible with a robust 5-fraction IMPT plan, compared to 20% for the robust reference plan.

The cumulative EQD7.04 distribution remains widely homogeneous within the target volume despite range errors and the sparing of the spinal cord is preserved (Figures 3d-f). Note that, the robust combined plan offers better target coverage than the single-modality IMPT plan for all range error scenarios. Figures 3e and 3f show that the target DVH of the single-modality IMPT plan deteriorates noticeably despite the use of robust planning. Finally, the DVHs show that the robustly optimized combination improves on the reference plan in the low dose region of the healthy tissues.

3.2. Sacral chordoma case

For the sacral chordoma case, the optimized combinations shown in Figure 4 for the nominal scenario use 10 IMPT and 20 IMRT fractions. In the non-robust optimized combination, on average a proton fraction delivers a fourfold dose to the GTV compared to a photon fraction (Figures 4a and 4b). Consequently, the total dose delivered with photons is reduced and the optimized combination achieves 92% of mean BED reduction in the bowel that is possible with a 30-fractions IMPT plan. The same mean bowel dose reduction requires 28 proton fractions in a simple proportional combination of IMRT and IMPT plans.

The hypofractionation of the GTV with protons comes with a small deviation from uniform fractionation in the region where the bowel and PTV overlap. In fact, photons and protons

deliver approximately 1.4 Gy and 2.5 Gy, respectively. This generally leads to underdosing the PTV in this region. However, the resulting PTV underdosing is small and, by construction, not higher than in the reference plan. Figure 4c shows the cumulative EQD1.8 for the non-robust optimized combination. Figures 4d and 4e show how the IMRT and IMPT dose distributions per fraction are modified in the nominal case when range uncertainties are directly accounted for in treatment plan optimization. Robust planning avoids placing hot proton dose spots in front of the bowel. On average a photon fraction delivers a higher dose to the GTV than in the non-robust combination. Therefore, a smaller mean BED reduction in the bowel is expected. However, both the robust and non-robust optimized combinations achieve 92% of the integral dose reduction in the gastrointestinal tract that is possible with the single-modality IMPT plans.

Comparisons of the DVHs evaluated for the cumulative EQD1.8 from all robust and non-robust plans are shown in Appendix B for each error scenario. The values of the mean BED in the bowel from all plans are shown in Table 1 for the nominal scenario.

3.3. Atypical meningioma case

For the atypical meningioma case, non-robust multi-modality treatment planning leads to the optimized combination shown in Figures 5a-c for the nominal scenario. The plan uses 10 IMPT and 20 IMRT fractions. The IMRT and IMPT dose distributions per fraction are shown in Figures 5a and 5b. Near-uniform fractionation is achieved in the region where serial OARs overlay the PTV and in the peripheral parts of the PTV. Meanwhile, hypofractionation of the GTV with protons allows achieving 48% of mean BED reduction in the normal brain that is possible with a 30-fractions IMPT plan (compared to 33% for the reference plan).

Robust multi-modality treatment planning yields the solution shown in Figures 5d-f for the nominal scenario. Robustness against range uncertainties is achieved without compromising the benefit of the optimized combination over the reference plan. In fact, the robust optimized combination achieves 46% of mean BED reduction in the normal brain that is possible with a robust 30-fractions IMPT plan (compared to 33% for the reference plan).

Comparisons of the DVHs evaluated for the cumulative EQD1.8 from all robust and non-robust plans are shown in Appendix B for each error scenario. Values of the mean BED in the healthy tissues from all plans are shown in Table 1 for the nominal scenario.

4. Discussion and conclusions

Due to the high cost of establishing and maintaining proton therapy centers, proton treatment slots are still a limited resource. Recently, combined proton-photon treatments in which most fractions are delivered with photons and only a few with protons have been investigated as an approach to optimally make use of limited proton slots [8]. When serial OARs are located within or near the tumor, the optimal multi-modality treatment is a non-trivial combination of IMRT and IMPT plans. The proton fractions hypofractionate parts of the tumor while near-uniform fractionation is maintained in dose-limiting normal tissues to exploit the fractionation effect. Thus, IMRT fractions are primarily used to treat the region where the target volume and OARs overlay, and consequently, the photon dose bath in healthy tissues surrounding the tumor is reduced compared to naïve combinations.

Our work shows that the quality of such non-trivial combinations of proton and photon plans may be highly compromised if protons range errors are not accounted for during multi-modality treatment planning. However, robust combined treatment plans can be obtained via stochastic

optimization. Robustness against range uncertainties may reduce the benefit of optimal combinations over simple combinations of IMRT and IMPT plans. However, a substantial benefit remains. In certain situations, a photon component in a combined treatment can even improve treatment plan robustness compared to robustly optimized single-modality IMPT plans.

In addition to range errors, robustness against setup errors is of crucial importance for combined proton-photon treatments. In this work, we consider a hybrid planning approach in which we apply stochastic optimization to range uncertainties only, while accounting for other potential sources of error through safety margins. Such an approach was also considered by Tommasino *et al* [18] for the robust multi-field optimization of proton plans and it was found that the hybrid technique allows obtaining the same plan quality as full robust optimization without worsening the robustness to setup errors. Figure 6 evaluates the sensitivity of the combined proton-photon spinal metastasis plan that is robust to range uncertainties (Figures 2l-n) against systematic setup errors. The dose distribution from the robustly optimized combined plan with respect to range errors was recalculated for shifts of $\pm$3mm in the 3 cardinal directions (CC, AP, and RL). Setup errors were modelled as a shift in the treatment isocenter position. We distinguish two cases for the robustness evaluation against setup errors: 1) systematic shifts that apply to all proton and photon fractions in the same way, and 2) shifts that lead to a misalignment of proton and photon dose contributions, i.e. a different systematic shift is applied to proton and photon fractions. Figure 6a shows that the sensitivity to a systematic setup error that affects photon and proton fractions the same way is comparable to that of IMRT-only plans. No difference in sparing the spinal cord is seen between the IMRT-only plan (faint dotted lines) and the combined proton-photon plan (solid lines). In this regard, little gain is expected from handling setup errors through robust planning rather than margins [13].

However, combined treatments may be very sensitive to misalignments of the proton and photon distributions. This is illustrated in Figure 6b, which shows the degradation of the dose homogeneity in the CTV for such error scenarios (faint lines). In this situation, robust optimization could be used to improve the robustness of combined treatment plans, which is expected to result in smoother dose gradients in the photon and proton dose contributions within the CTV. While most commercial IMPT treatment planning systems support robust optimization for systematic setup errors that equally apply to all fractions, the application to misaligned proton and photon doses in combined treatments is computationally more demanding. It requires including the combination of different setup errors as additional error scenarios, and thus requires additional research.

Recently, also other groups have investigated the optimization of combined proton-photon treatment plans [7, 10]. Here, we comment on differences in our work. Ten Eikelder *et al* [7] consider IMRT treatment plans and passive scattering based proton plans for liver cancer patients, which are separately planned. Given the dose distributions of these plans, BED criteria are used to optimize the number of fractions and the dose per fraction for the proton and photon plans. Gao [10] simultaneously optimize IMRT and IMPT plans while accounting for range and setup errors through stochastic optimization, but joint optimization is performed based on cumulative physical dose rather than BED. As this method does not account for fractionation, additional objectives are introduced to enforce that both modalities individually deliver homogeneous doses to the target volume so that the final dose distribution can approximately be divided into proton and photon fractions. The main difference to our work is that both of these works consider treatments in which protons and photons individually deliver homogeneous doses to the target volume. In the approach of ten Eikelder *et al*, the dose per fraction for protons could be increased uniformly to all

of the target volume if the proton plan was superior to the photon plan but the number of available proton fractions was limited. This is often the case for liver tumors as considered by ten Eikelder *et al*. However, if serial dose-limiting normal tissues overlay the target volume as in the three examples considered in this paper, their approach is limited. In that regard, the method proposed here represents an extension that allows for increasing the proton dose per fraction only in parts of the target. The work by Gao (and also ten Eikelder *et al*) is motivated by the assumption that protons and photons have complementary advantages regarding different aspects of the dose distribution and their sensitivity to uncertainties. In our work, combined proton-photon treatments are instead motivated by the limited availability of proton fractions rather than a dosimetric advantage of the photon component. The goal is, therefore, to deliver an overproportioned dose with protons to parts of the target. This leads to inhomogeneous proton and photon dose contributions, which adds to the complexity of robustness evaluation and optimization. In Gao's approach, the robustness of the photon and proton components is instead similar to that of single modality IMRT and IMPT plans.

In addition, we want to comment on the following aspects:

- In this work, the dose distributions of IMRT and IMPT fractions are jointly optimized whereas the number of proton fractions is preset. The number of proton fractions per patient is not decided based on plan quality for the individual patient. Instead, combining protons and photons is motivated here by limited proton resources. The long term goal is to maximize the benefit of proton therapy over the entire patient population by optimizing the allocation of proton slots over the patient cohort. As a next step towards this goal, the benefit of combined proton-photon treatments for individual patients can be studied as a function of the number of proton fractions. This has been discussed elsewhere [8].

- In this paper, we suggest combined treatments where the dose per fraction is not uniform within the target volume and varies between proton and photon fractions. We assume that the BED formalism can be extended to describe the fractionation effects in this situation. We further use the same $^{\alpha}/_{\beta}$-ratios for the two different radiation modalities, which is motivated by the fact that the same fractionation schemes are used for both protons and photons in current clinical practice. An additional concern of the BED model is that the $^{\alpha}/_{\beta}$-ratios are uncertain. However, we show that the benefit of combined proton-photon treatments varies weakly with the $^{\alpha}/_{\beta}$-ratio within the range of typically assumed values (see Appendix C).
- Many extensions of the BED model have been proposed to incorporate higher-order radiobiological effects such as variable RBE of protons, repopulation, and reoxygenation [19, 21-25]. Using extended BED models for plan optimization could in principle incorporate these effects in the design of combined proton-photon treatments. In this study, we used the BED model in its basic form, which implies that the order of the proton and photon fractions does not matter. There exist BED model extensions in which the response to radiation depends on the individual doses per fraction and their order [26]. Such models would potentially have an impact on the design of combined treatments, however, these models are not established in clinical practice and are thus not considered here. Without a major shift in the clinical paradigm, the order of protons and photon fractions may be decided such to deliver the prescribed dose per week at the end of every week.

References

1. Durante M and Paganetti H, *Nuclear physics in particle therapy: a review.* Rep Prog Phys 2016. **79**(9): p. 59.
2. Langendijk JA, et al., *Selection of patients for radiotherapy with protons aiming at reduction of side effects: the model-based approach.* Radiother Oncol, 2013. **107**: p. 267-273.
3. Glimelius B, et al., *Number of patients potentially eligible for proton therapy.* Acta Oncol, 2005. **44**(8): p. 836-849.
4. Delaney AR, et al., *Using a knowledge-based planning solution to select patients for proton therapy.* Radiother Oncol, 2017. **124**(2): p. 263-270.
5. Hug EB, et al., *Locally challenging osteo- and chondrogenic tumors of the axial skeleton: results of combined proton and photon radiation therapy using three-dimensional treatment planning.* Int J Radiat Oncol Biol Phys, 1995. **31**(3): p. 467-476.
6. Boskos C, et al., *Combined proton and photon conformal radiotherapy for intracranial atypical and malignant meningioma.* Int J Radiat Oncol Biol Phys, 2009. **75**(2): p. 399-406.
7. ten Eikelder SCM, et al., *Optimal combined proton-photon therapy schemes based on the standard BED model.* Phys Med Biol, 2019. **64**: p. 21
8. XXX.
9. Feuvret L, et al., *A treatment planning comparison of combined photon-proton beams versus proton beams-only for the treatment of skull base tumors.* Int J Radiat Oncol Biol Phys, 2007. **69**: p. 944-954.
10. Gao, H., *Hybrid proton-photon inverse optimization with uniformity-regularized proton and photon target dose.* Phys Med Biol, 2019. **64**: p. 11.

11. Unkelbach J, Chan TCY, and Bortfeld T, *Accounting for range uncertainties in the optimization of intensity modulated proton therapy.* Phys Med Biol, 2007. **52**: p. 2755-2773.
12. Unkelbach J, et al., *Reducing the sensitivity of impt treatment plans to setup errors and range uncertainties via probabilistic treatment planning.* Med Phys, 2009. **36**: p. 149-163.
13. Unkelbach J, et al., *Robust radiotherapy planning.* Phys Med Biol, 2018. **63**: p. 28.
14. Fredriksson A, Forsgren A, and Hårdemark B, *Minimax optimization for handling range and setup uncertainties in proton therapy.* Med Phys, 2011. **38**(3): p. 1672-1684.
15. Fredriksson A, *A characterization of robust radiation therapy treatment planning methods-from expected value to worst case optimization.* Med Phys, 2012. **39**(8): p. 5169-5181.
16. Liu W, et al., *Robust optimization of intensity modulated proton therapy.* Med Phys, 2012. **39**(2): p. 1079-1091.
17. Pflugfelder D, Wilkens JJ, and Oelfke U, *Worst case optimization: a method to account for uncertainties in the optimization of intensity modulated proton therapy.* Phys Med Biol, 2008. **53**(6): p. 1689-1700.
18. Tommasino F, et al., *Clinical implementation in proton therapy of multi-field optimization by a hybrid method combining conventional PTV with robust optimization.* Phys Med Biol, 2020. **65**: p. 14.
19. Fowler JF, *21 years of biologically effective dose.* Br J Radiol, 2010. **83**: p. 554-568.
20. Unkelbach J and Paganetti H, *Robust proton treatment planning: physical and biological optimization.* Semin Radiat Oncol, 2018. **28**: p. 86-96.
21. Travis EL and Tucker SL, *Isoeffect models and fractionated radiation therapy.* Int J Radiat Oncol Biol Phys, 1987. **13**(2): p. 283-287.

22. van de Geijn J, *Incorporating the time factor into the linear-quadratic model.* Br J Radiol, 1989. **62**(735): p. 296-298.

23. Hall EJ and Giaccia AJ, *Radiobiology for the Radiobiologist*. 2006, Philadelphia.

24. Paganetti H, *Relative biological effectiveness (RBE) values for proton beam therapy. Variations as a function of biological endpoint, dose, and linear energy transfer.* Phys Med Biol, 2014. **59**(22): p. R419-472.

25. Tommasino F and Durante M, *Proton radiobiology.* Cancers (Basel), 2015. **7**(1): p. 353-381.

26. Kehwar TS, et al., *Accelerated proliferation correction factors in linear-quadratic and multiple-component models.* Iran J Radiat Res, 2007. **5**(2): p. 53-61.

Figure captions

Figure 1: (a) Patient with spinal metastasis. The contours show the PTV (black), the cauda (red), and the corresponding PRV (light blue). (b) Patient with a sacral chordoma. The contours show the GTV (blue), CTV (dark green), PTV (black), and bowel (purple). (c) Patient with an atypical meningioma. The contours show the GTV (blue), PTV (black), brainstem (magenta), optic nerves and pituitary gland (green).

Figure 2: Combined proton-photon plans for the spinal metastasis case in the nominal scenario: (a)-(c) non-robust reference plan; (d)-(f) non-robust optimized combination; (g)-(i) robust reference plan; (l)-(n) robust optimized combination. The IMPT plan uses 3 beams (gantry angles 135°, 180°, and 225°). Left panels: IMRT and IMPT dose distributions per fraction. Right panel: cumulative equieffective dose EQD7.04.

Figure 3: Comparison of the DVHs evaluated for the EQD7.04 from all 4 non-robust (top row) and robust (bottom row) plans for the nominal scenario [(a) and (d)], the undershoot [(b) and (e)], and overshoot [(c) and (f)] scenarios. Shown are the DVHs for the target (black), cauda (red), PRV (light blue), and healthy tissues (cyan).

Figure 4: Optimized proton-photon combinations for the sacral chordoma case in the nominal scenario. Top row: non-robust plan. Bottom row: robust plan. The IMPT plan uses 3 beams (gantry angles 0°, 45°, and 315°). [(a) and (d)] IMRT dose distribution per fraction; [(b) and (e)] IMPT dose distribution per fraction; [(c) and (f)] cumulative equieffective dose EQD1.8.

Figure 5: Optimized proton-photon combinations for the atypical meningioma case in the nominal

scenario. Top row: non-robust plan. Bottom row: robust plan. The IMPT plan uses 2 fields (60° and 140° gantry angles). [(a) and (d)] IMRT dose distribution per fraction; [(b) and (e)] IMPT dose distribution per fraction; [(c) and (f)] cumulative equieffective dose EQD1.8.

Figure 6: Sensitivity analysis against setup errors for the spinal metastasis case. Shown are the DVHs for the CTV (green), and cauda (red). (a) DVHs from the single modality IMRT plan (faint dotted lines) and nominal robust combined plan (solid lines) for 7 scenarios, corresponding to systematic 3 mm shifts of both proton and photon dose distributions. (b) DVHs from the robust combined plan in the nominal scenario (dashed lines) and in 48 scenarios, corresponding to systematic shifts of both proton and photon dose distributions (full lines) and misalignments between the two modalities (faint lines).

Table captions

Table 1: Summary of the mean BED values in the healthy tissues (for the spinal metastasis case and the atypical meningioma case) and bowel (for the sacral chordoma case) from the non-robust and robust single-modality IMRT and IMPT plans and proton-photon combinations for the nominal scenario.

	Mean BED [Gy]					
	spinal metastasis (healthy tissues)		sacral chordoma (bowel)		atypical meningioma (healthy tissues)	
Plan	**non-robust**	**robust**	**non-robust**	**robust**	**non-robust**	**robust**
IMRT	5.73	/	12.22	/	10.71	/
IMPT	2.92	3.02	5.03	6.30	6.17	6.38
ref. plan	5.16	5.19	9.82	10.25	9.20	9.26
opt. comb.	3.17	4.25	5.57	6.78	8.54	8.72

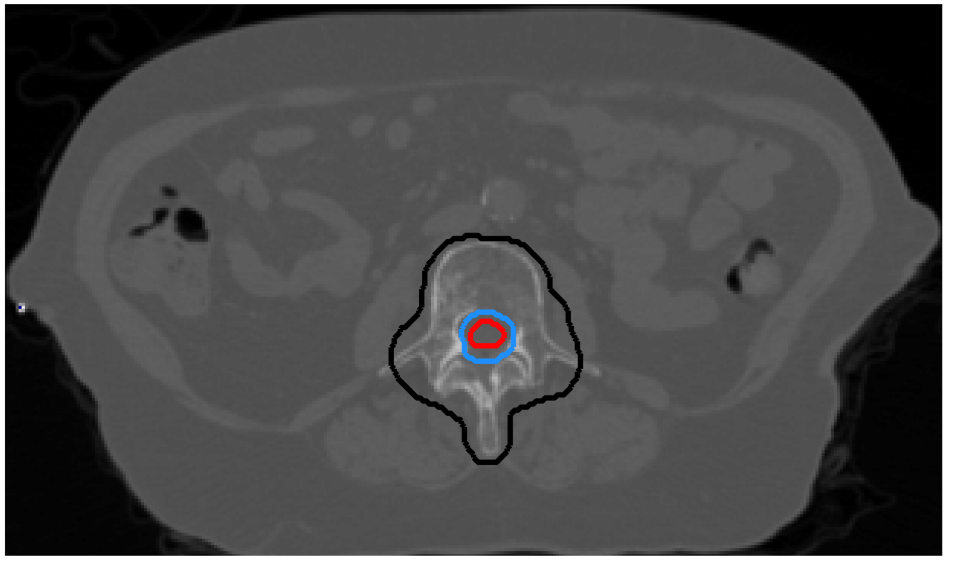

(a)

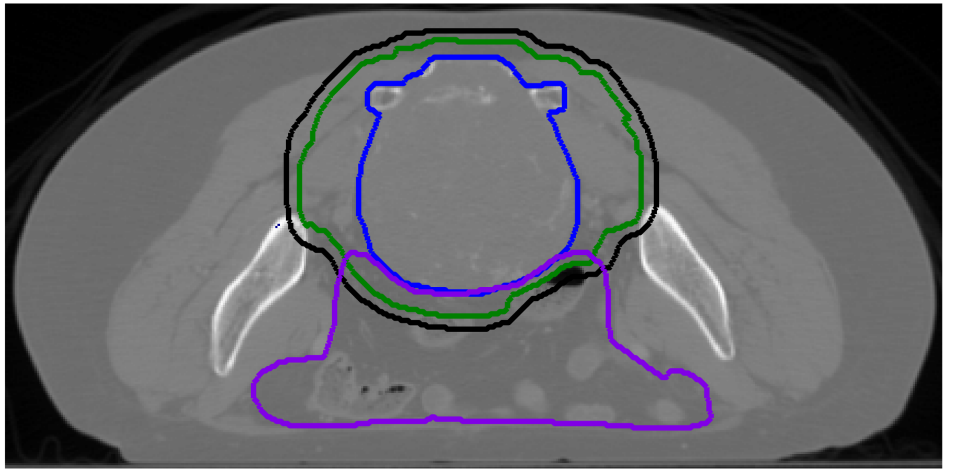

(b)

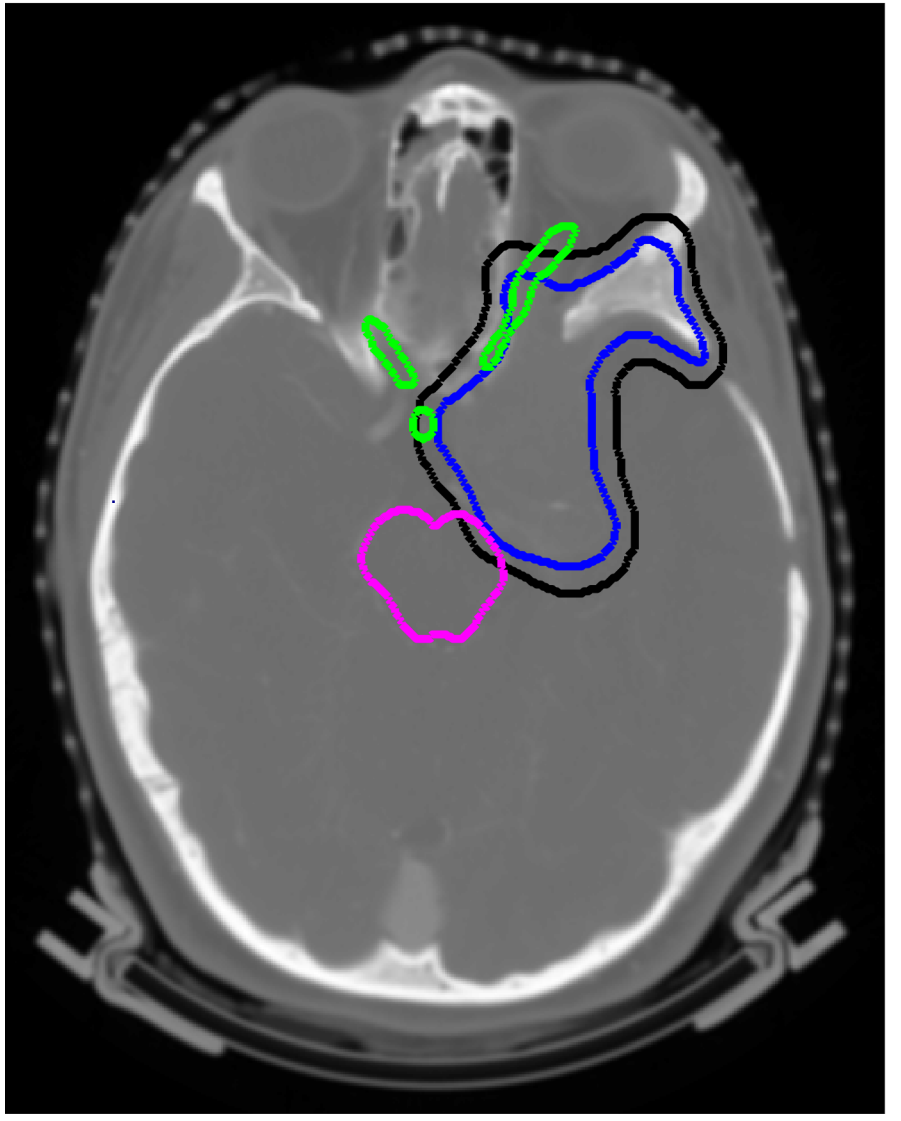

(c)

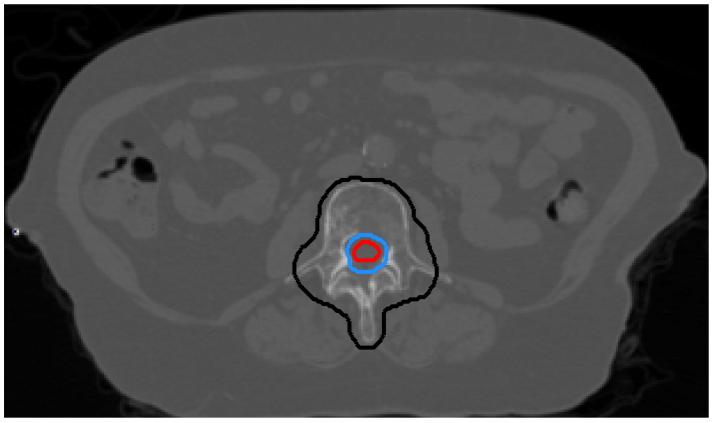

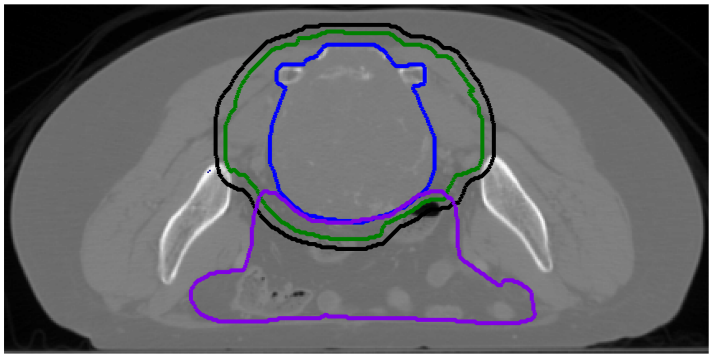

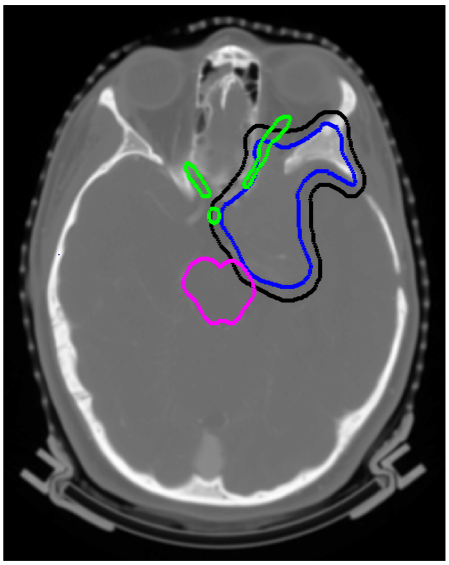

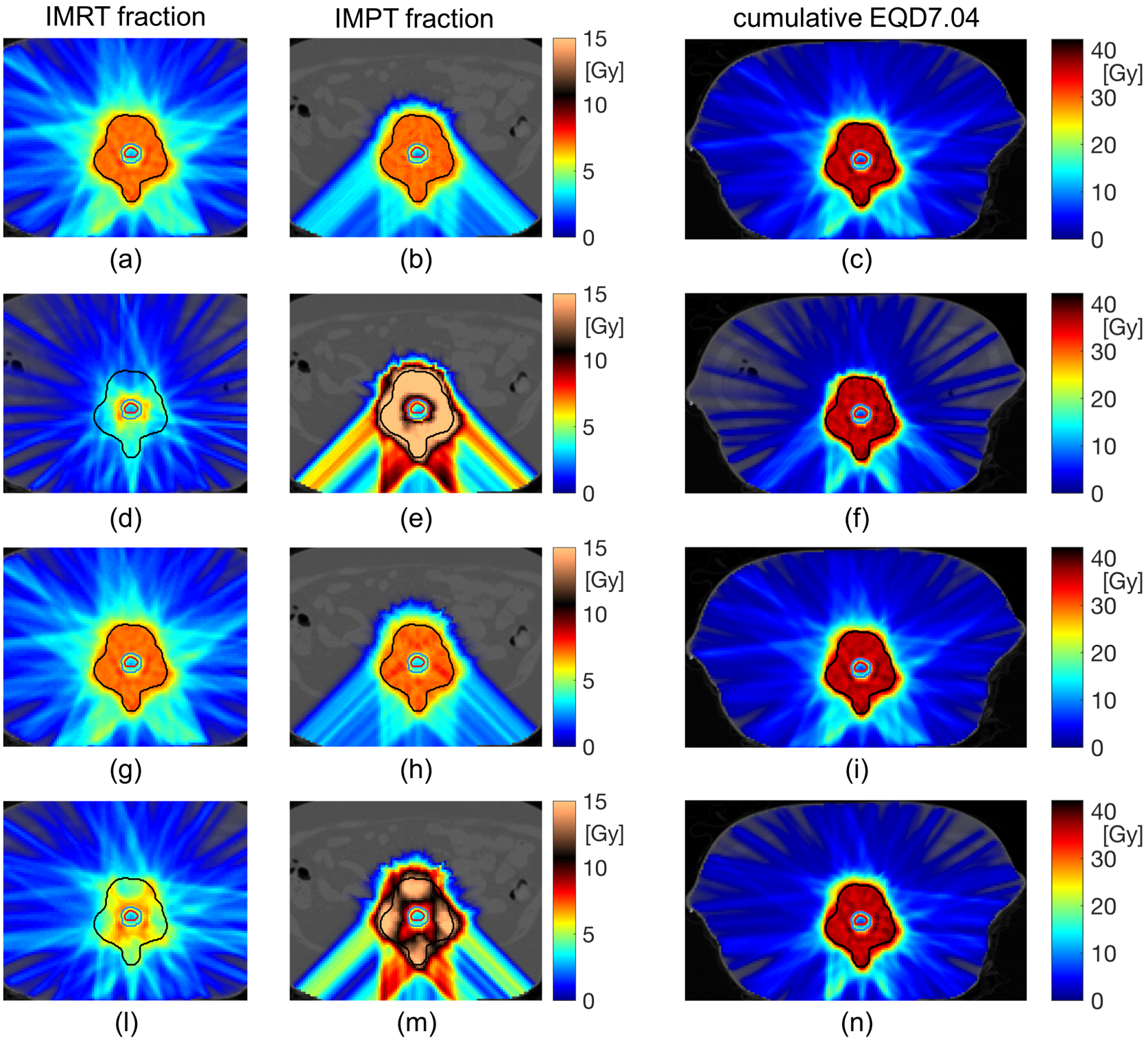
IMRT fraction
IMPT fraction
cumulative EQD7.04
15
[Gy]
10
5
0
40
[Gy]
30
20
10
0
(a)
(b)
(c)
(d)
(e)
(f)
(g)
(h)
(i)
(l)
(m)
(n)

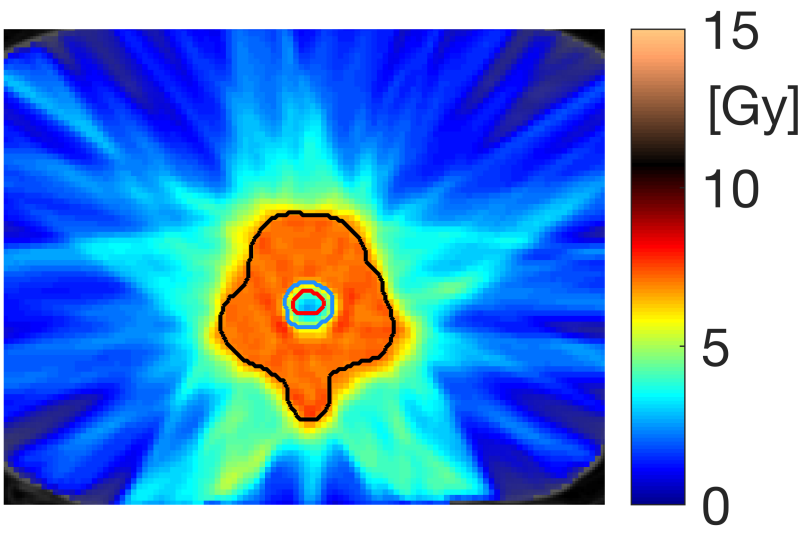
15
[Gy]
10
5
0

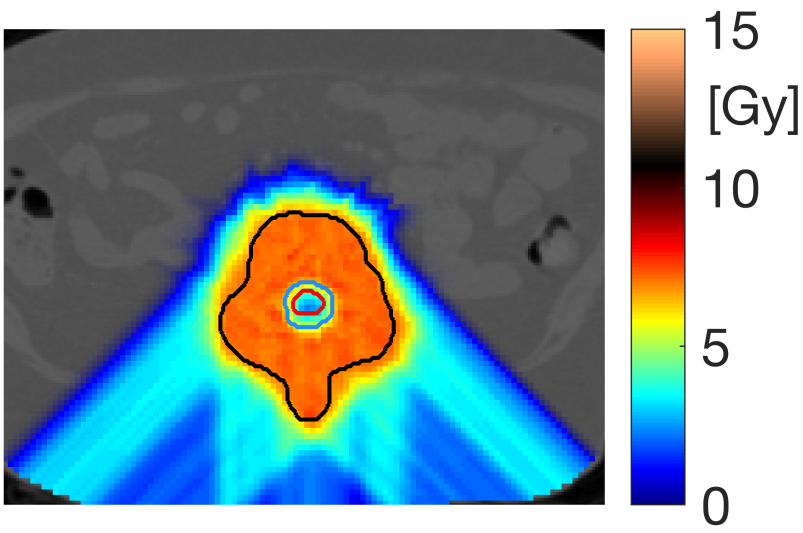
15
[Gy]
10
5
0

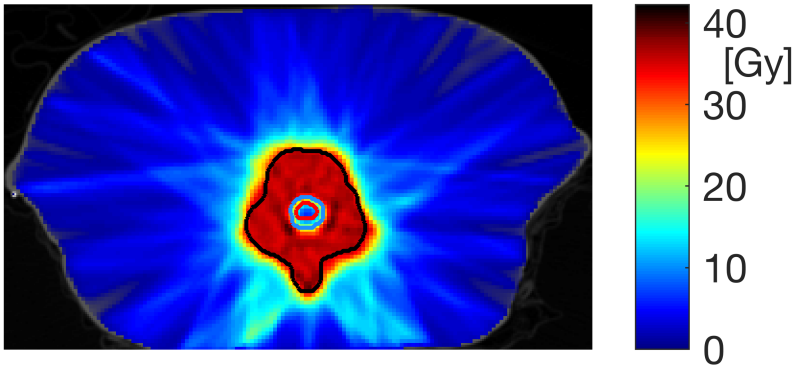
40
[Gy]
30
20
10
0

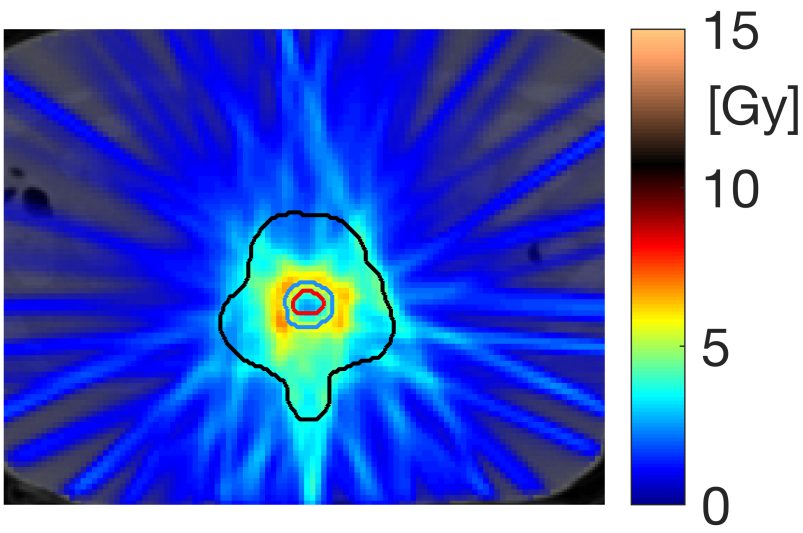
15
[Gy]
10
5
0

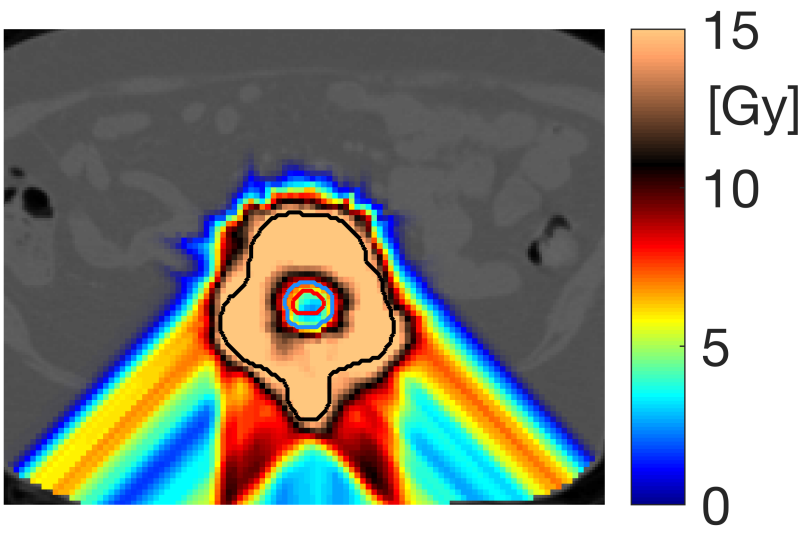
15
[Gy]
10
5
0

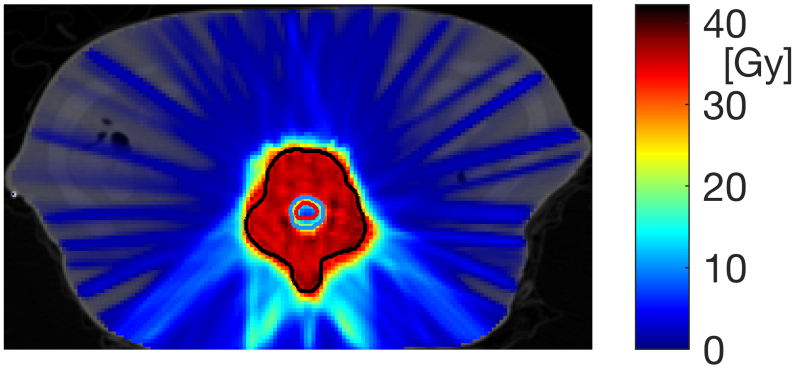
40
[Gy]
30
20
10
0

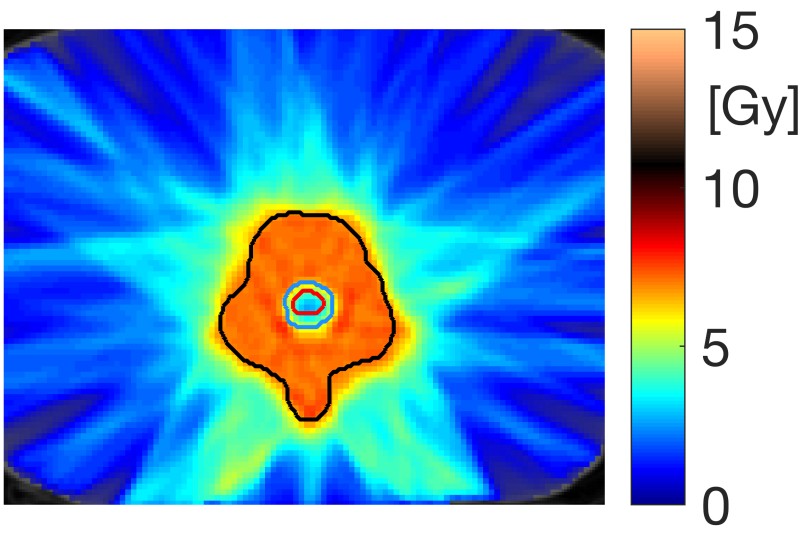
15
[Gy]
10
5
0

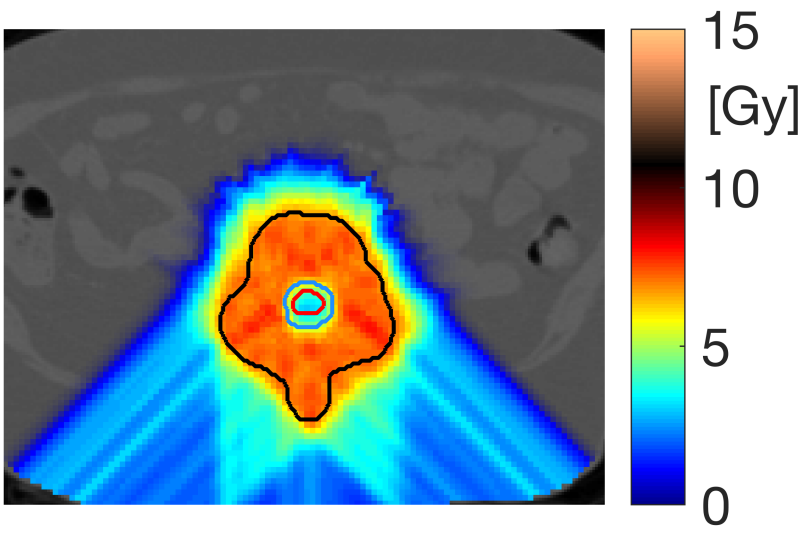
15
[Gy]
10
5
0

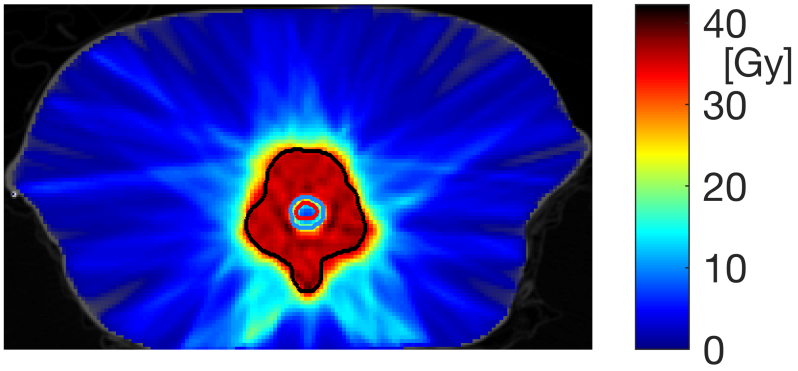
40
[Gy]
30
20
10
0

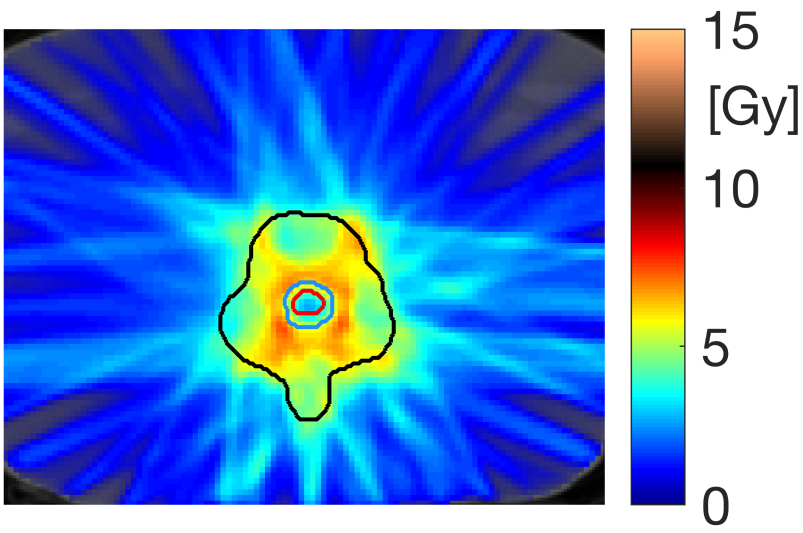
15
[Gy]
10
5
0

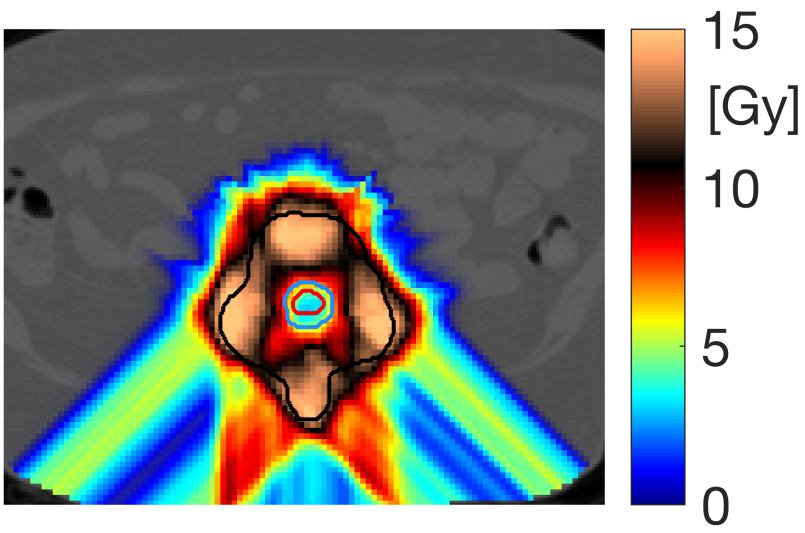
15
[Gy]
10
5
0

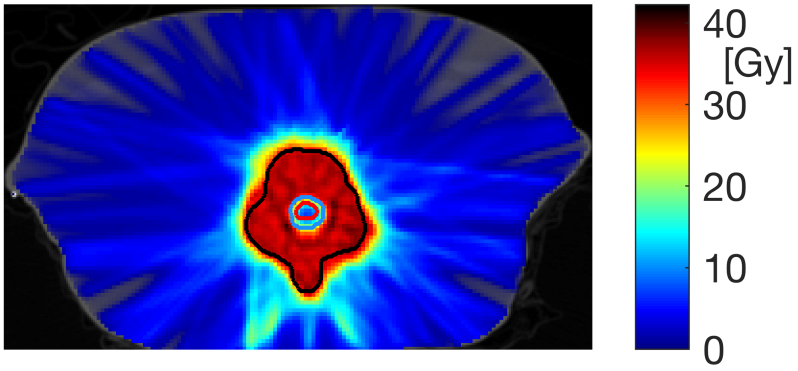
40
[Gy]
30
20
10
0

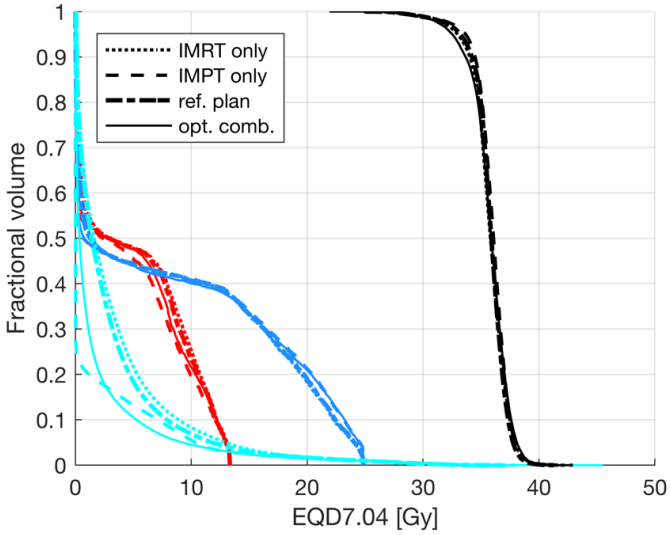
IMRT only
IMPT only
ref. plan
opt. comb.
Fractional volume
EQD7.04 [Gy]

(a)

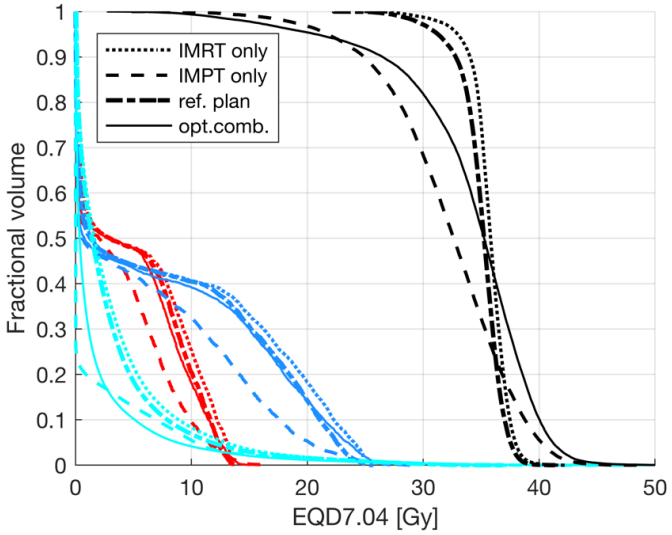
IMRT only
IMPT only
ref. plan
opt.comb.
Fractional volume
EQD7.04 [Gy]

(b)

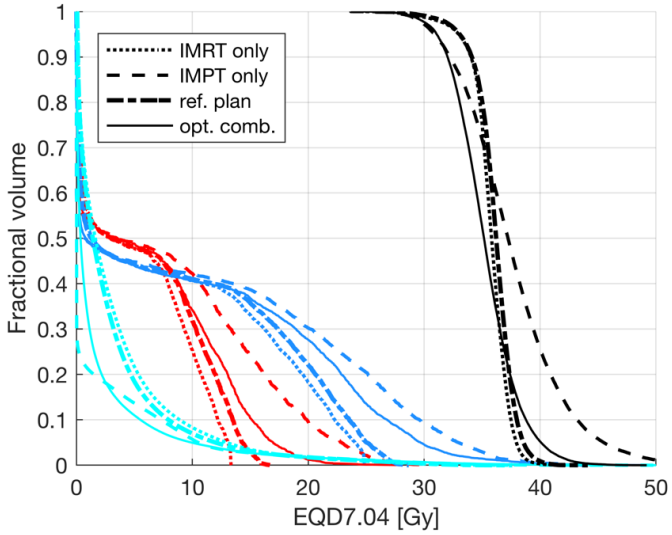
IMRT only
IMPT only
ref. plan
opt. comb.
Fractional volume
EQD7.04 [Gy]

(c)

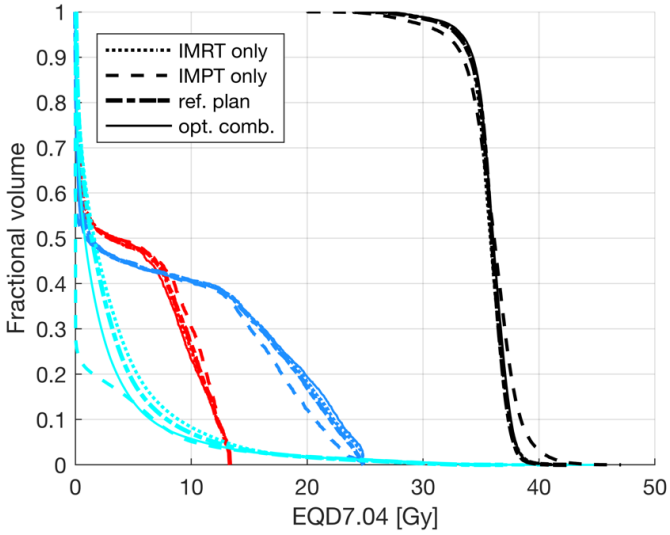
IMRT only
IMPT only
ref. plan
opt. comb.
Fractional volume
EQD7.04 [Gy]

(d)

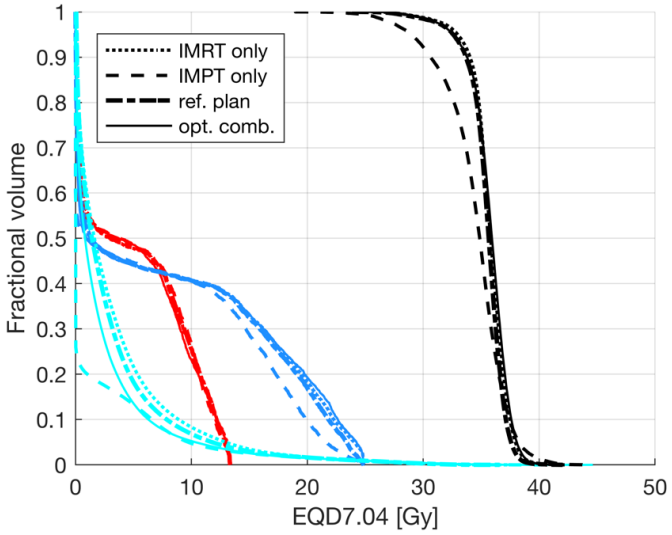
IMRT only
IMPT only
ref. plan
opt. comb.
Fractional volume
EQD7.04 [Gy]

(e)

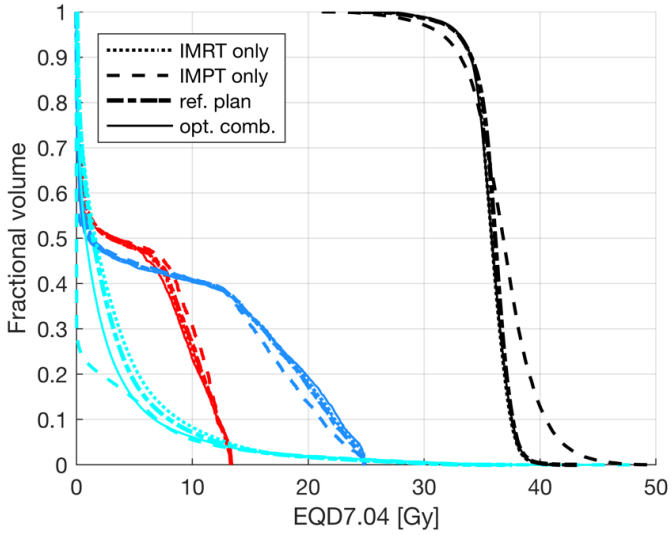
IMRT only
IMPT only
ref. plan
opt. comb.
Fractional volume
EQD7.04 [Gy]

(f)

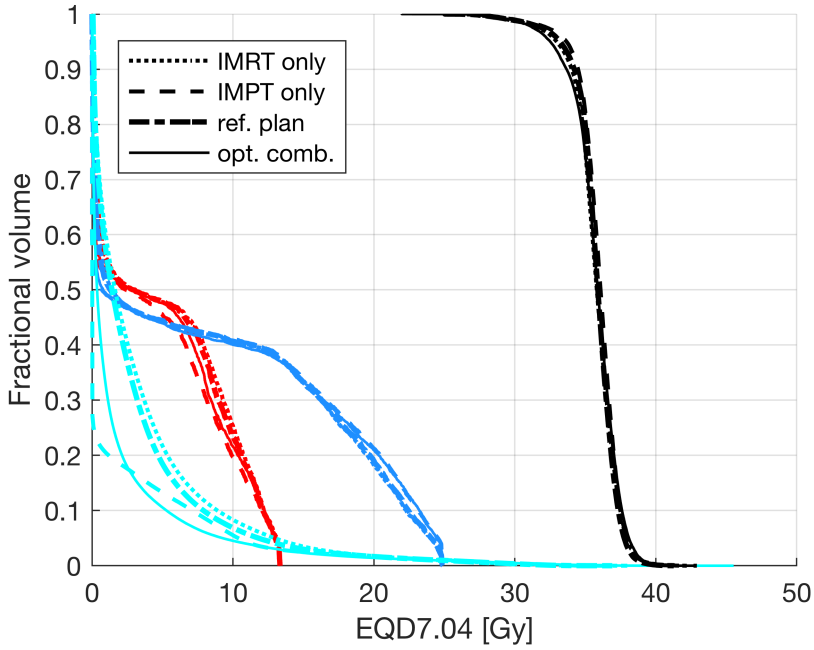
IMRT only
IMPT only
ref. plan
opt. comb.
Fractional volume
EQD7.04 [Gy]
0
0.1
0.2
0.3
0.4
0.5
0.6
0.7
0.8
0.9
1
0
10
20
30
40
50

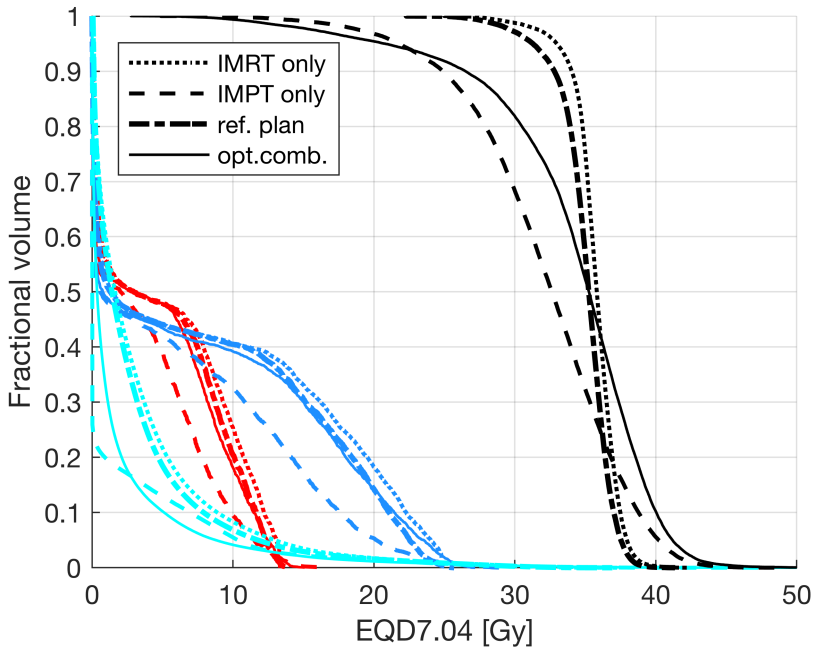
IMRT only
IMPT only
ref. plan
opt.comb.
Fractional volume
EQD7.04 [Gy]
0
0.1
0.2
0.3
0.4
0.5
0.6
0.7
0.8
0.9
1
0
10
20
30
40
50

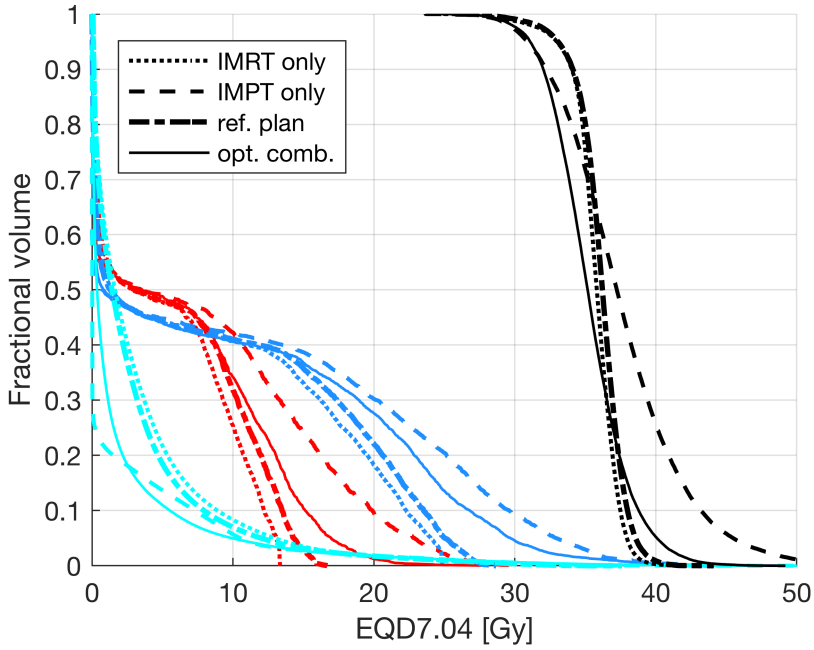
IMRT only
IMPT only
ref. plan
opt. comb.
Fractional volume
EQD7.04 [Gy]
0
0.1
0.2
0.3
0.4
0.5
0.6
0.7
0.8
0.9
1
0
10
20
30
40
50

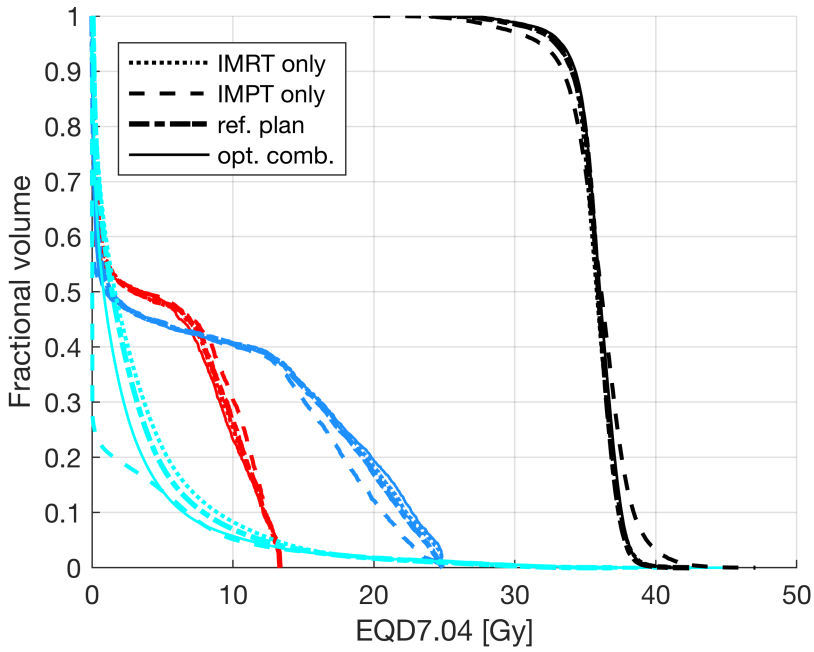
IMRT only
IMPT only
ref. plan
opt. comb.
Fractional volume
EQD7.04 [Gy]
0
0.1
0.2
0.3
0.4
0.5
0.6
0.7
0.8
0.9
1
0
10
20
30
40
50

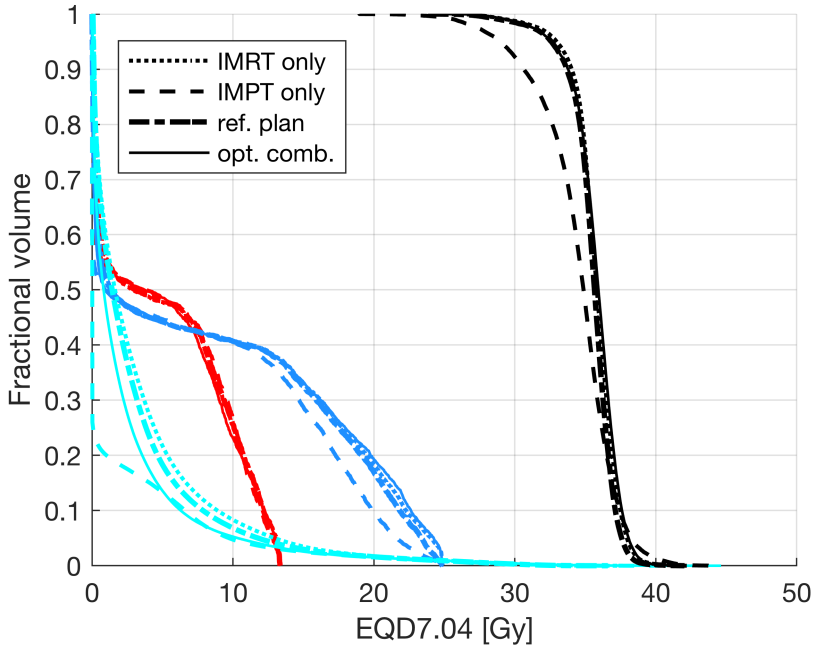
IMRT only
IMPT only
ref. plan
opt. comb.
Fractional volume
EQD7.04 [Gy]
0
0.1
0.2
0.3
0.4
0.5
0.6
0.7
0.8
0.9
1
0
10
20
30
40
50

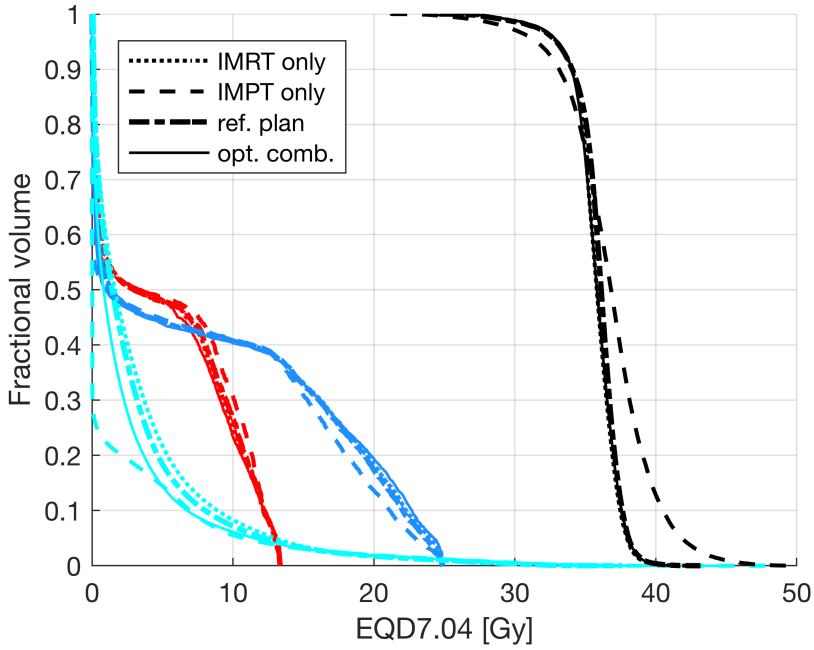
IMRT only
IMPT only
ref. plan
opt. comb.
Fractional volume
EQD7.04 [Gy]
0
0.1
0.2
0.3
0.4
0.5
0.6
0.7
0.8
0.9
1
0
10
20
30
40
50

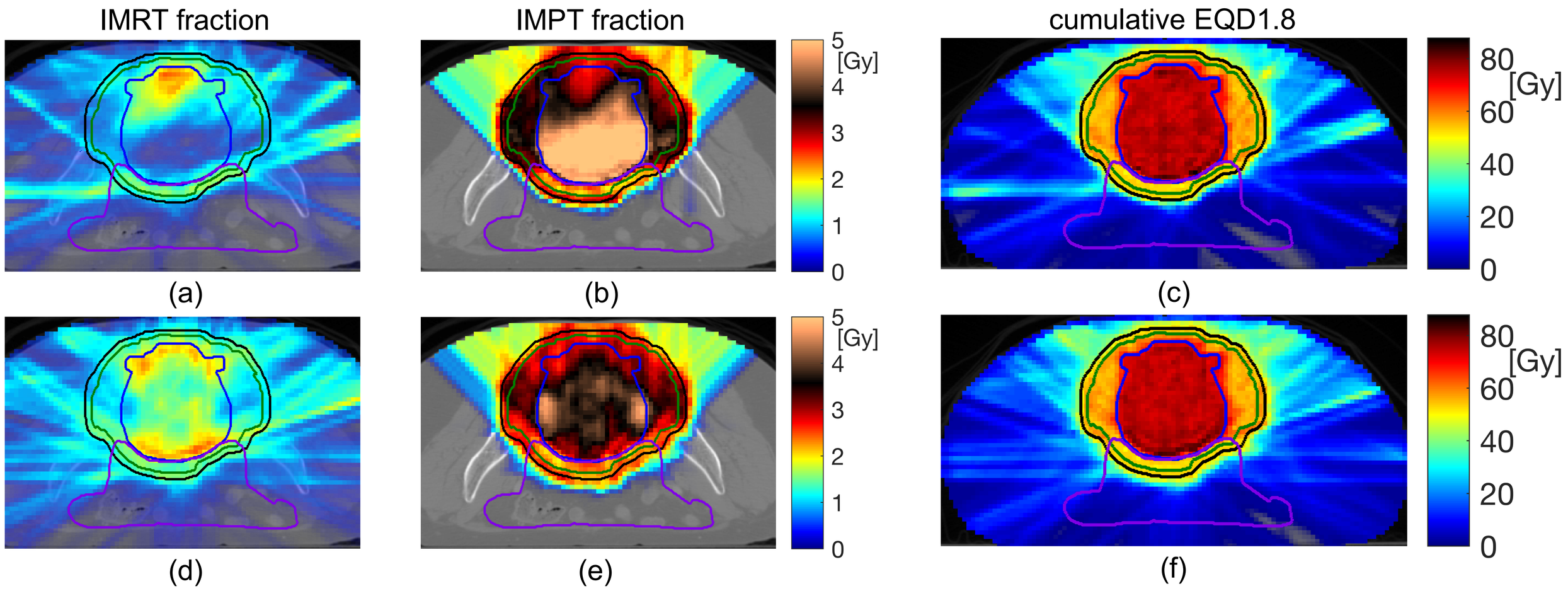
IMRT fraction
IMPT fraction
cumulative EQD1.8
5
[Gy]
4
3
2
1
0
80
[Gy]
60
40
20
0
(a)
(b)
(c)
(d)
(e)
(f)

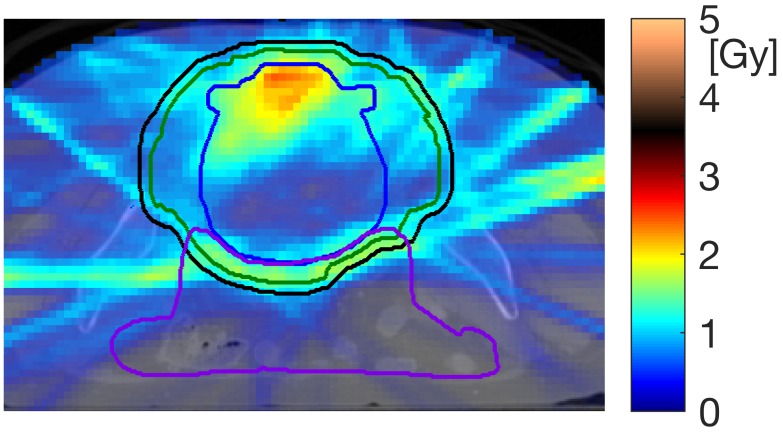
5
[Gy]
4
3
2
1
0

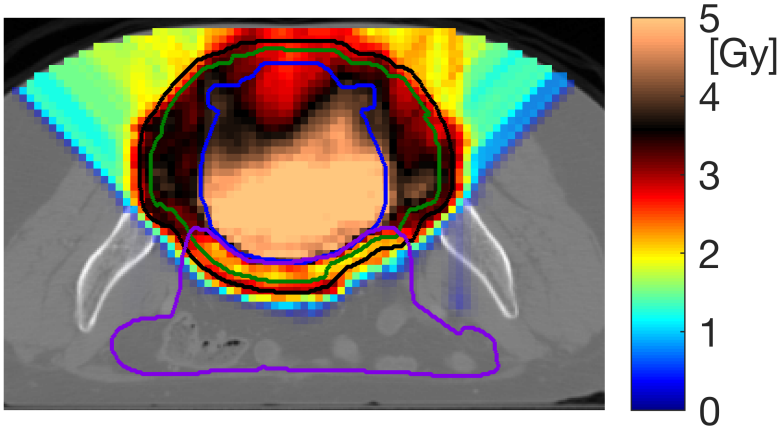
5
[Gy]
4
3
2
1
0

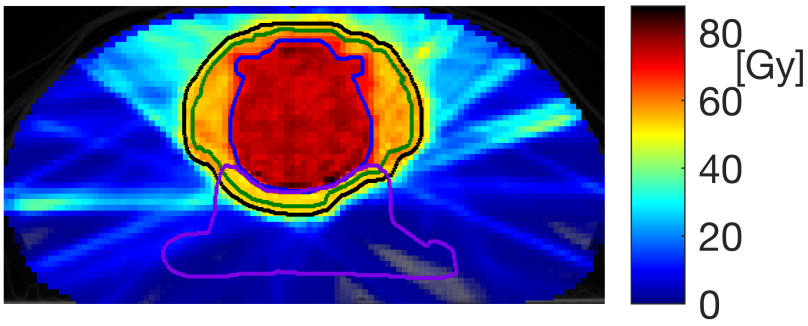
80
[Gy]
60
40
20
0

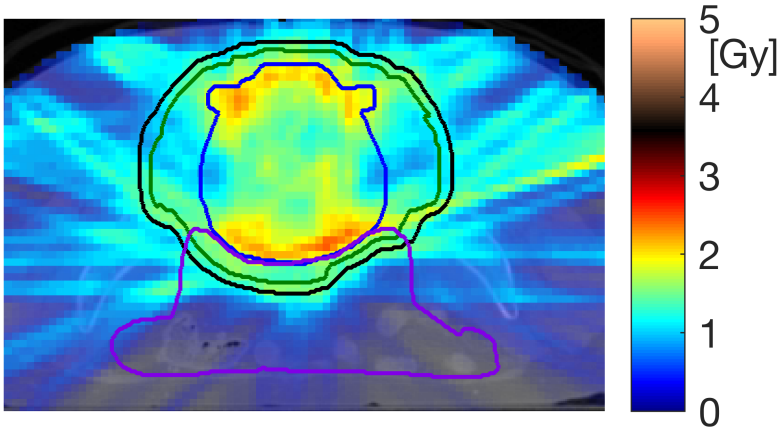
5
[Gy]
4
3
2
1
0

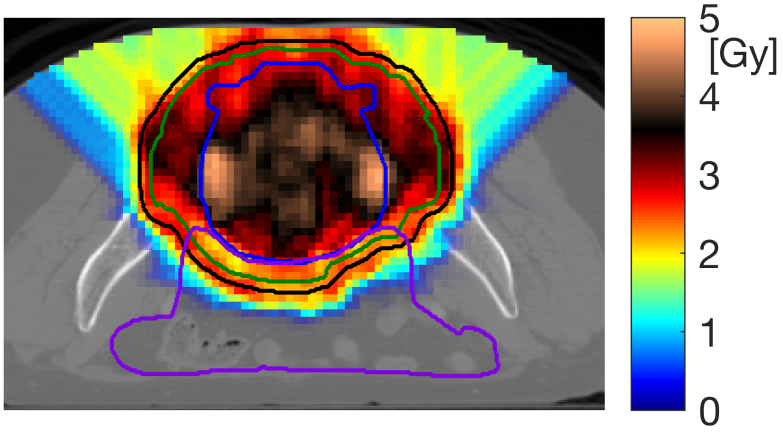
5
[Gy]
4
3
2
1
0

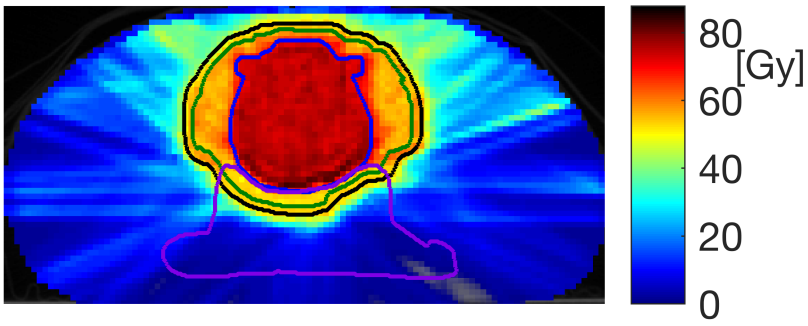
80
[Gy]
60
40
20
0

IMRT fraction

IMPT fraction

cumulative EQD1.8

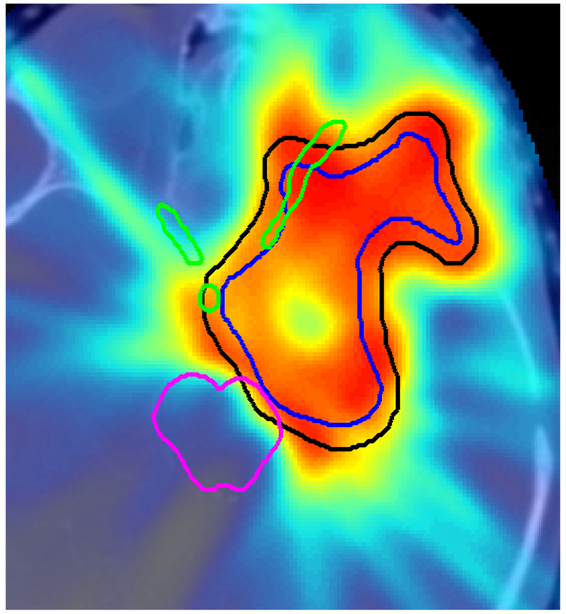

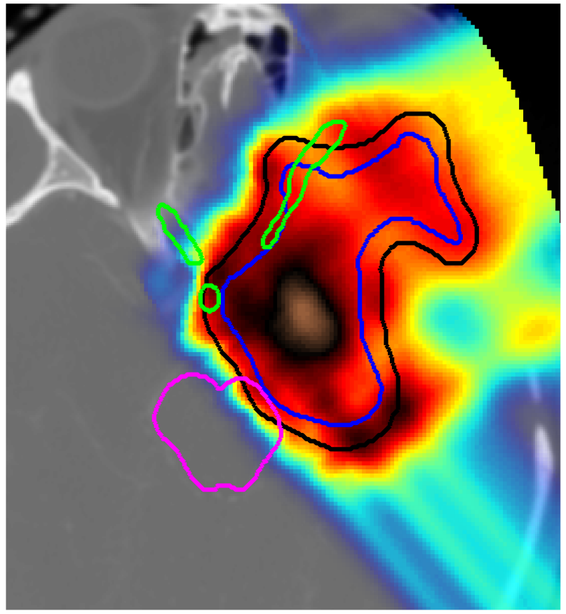

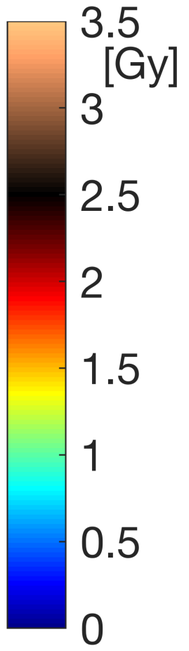

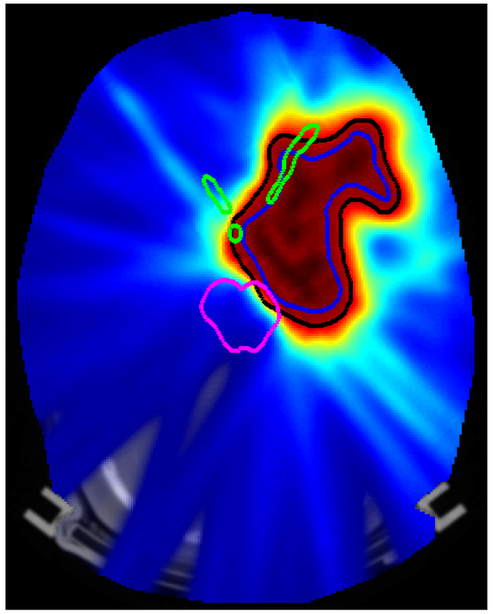

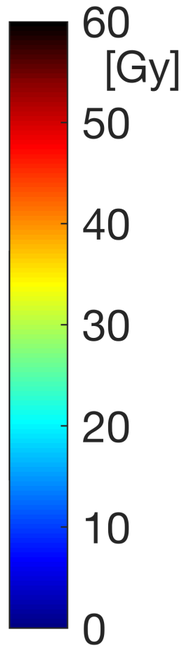

(a) (b) (c)

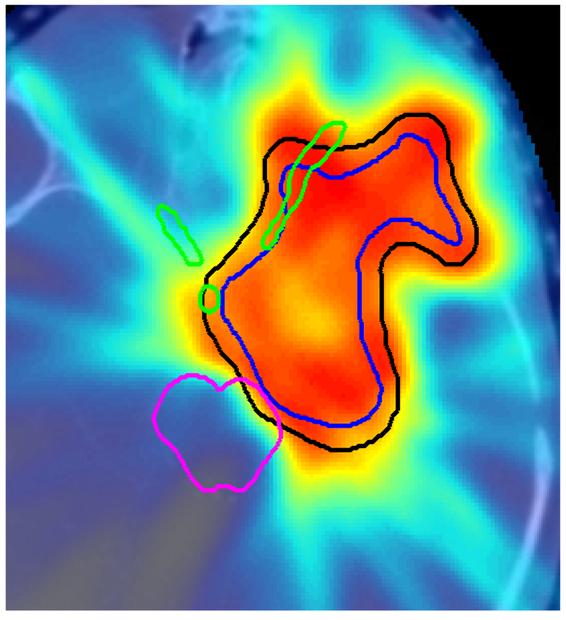

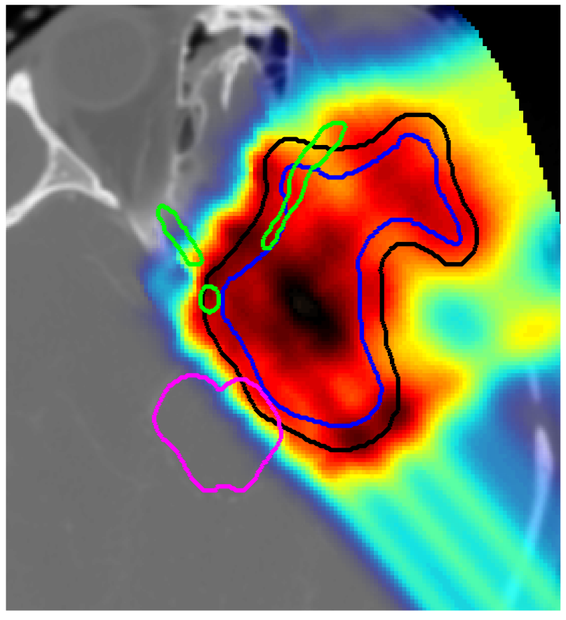

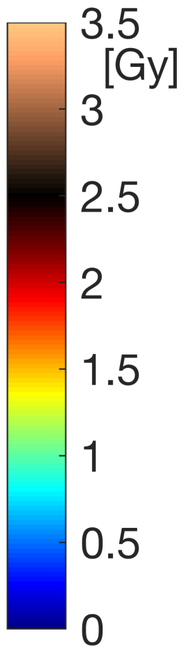

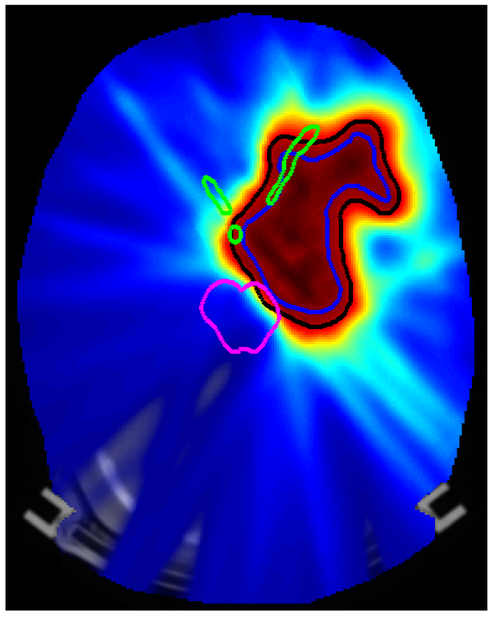

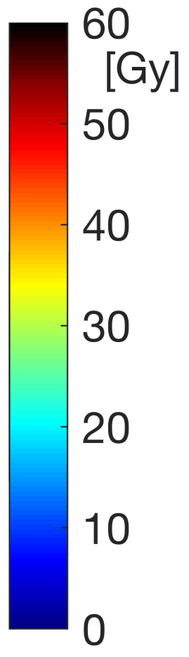

(d) (e) (f)

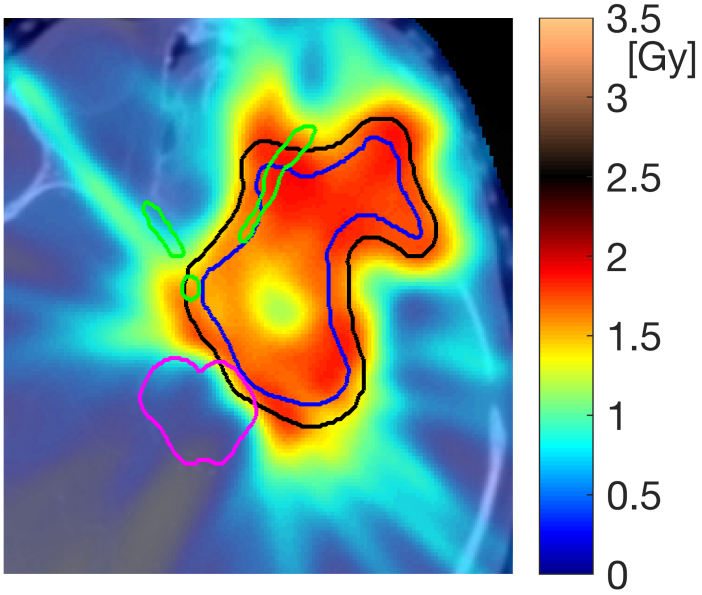
3.5
[Gy]
3
2.5
2
1.5
1
0.5
0

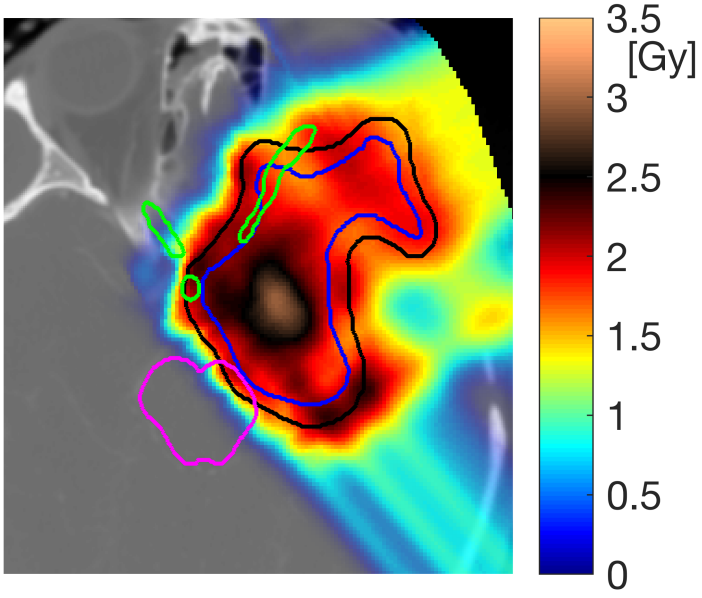
3.5
[Gy]
3
2.5
2
1.5
1
0.5
0

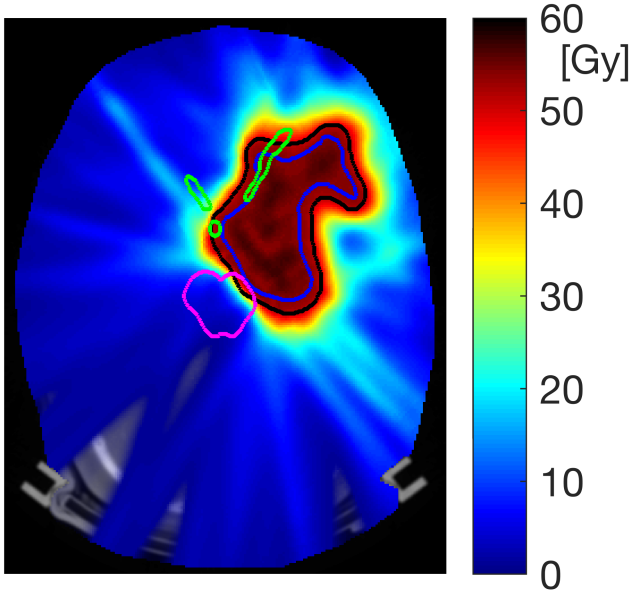
60
[Gy]
50
40
30
20
10
0

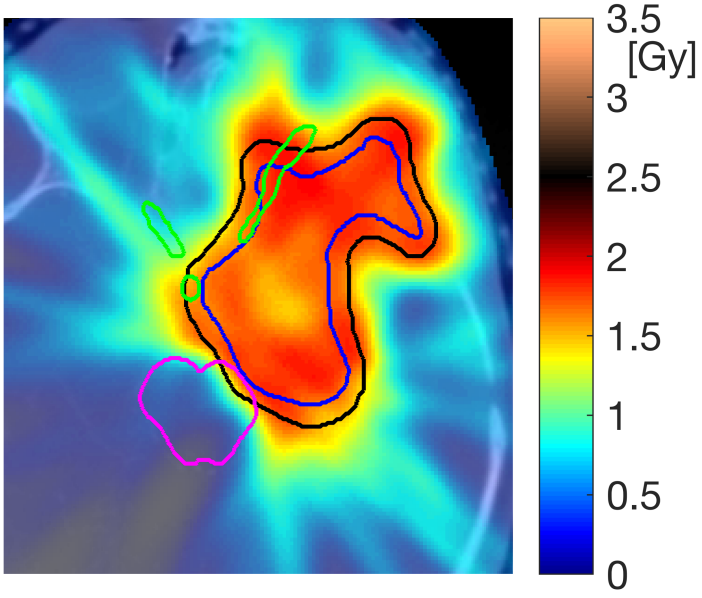
3.5
[Gy]
3
2.5
2
1.5
1
0.5
0

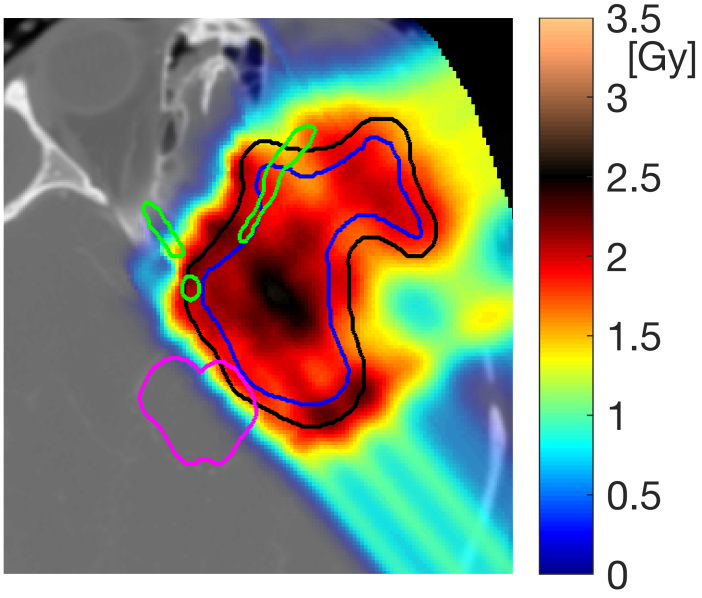
3.5
[Gy]
3
2.5
2
1.5
1
0.5
0

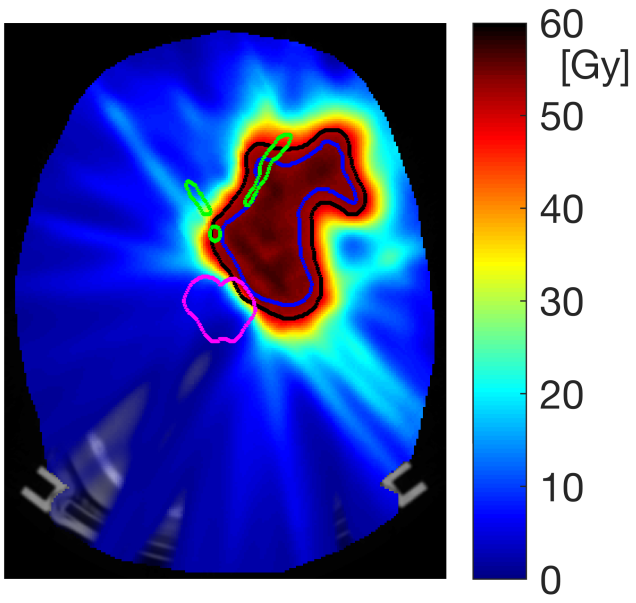
60
[Gy]
50
40
30
20
10
0

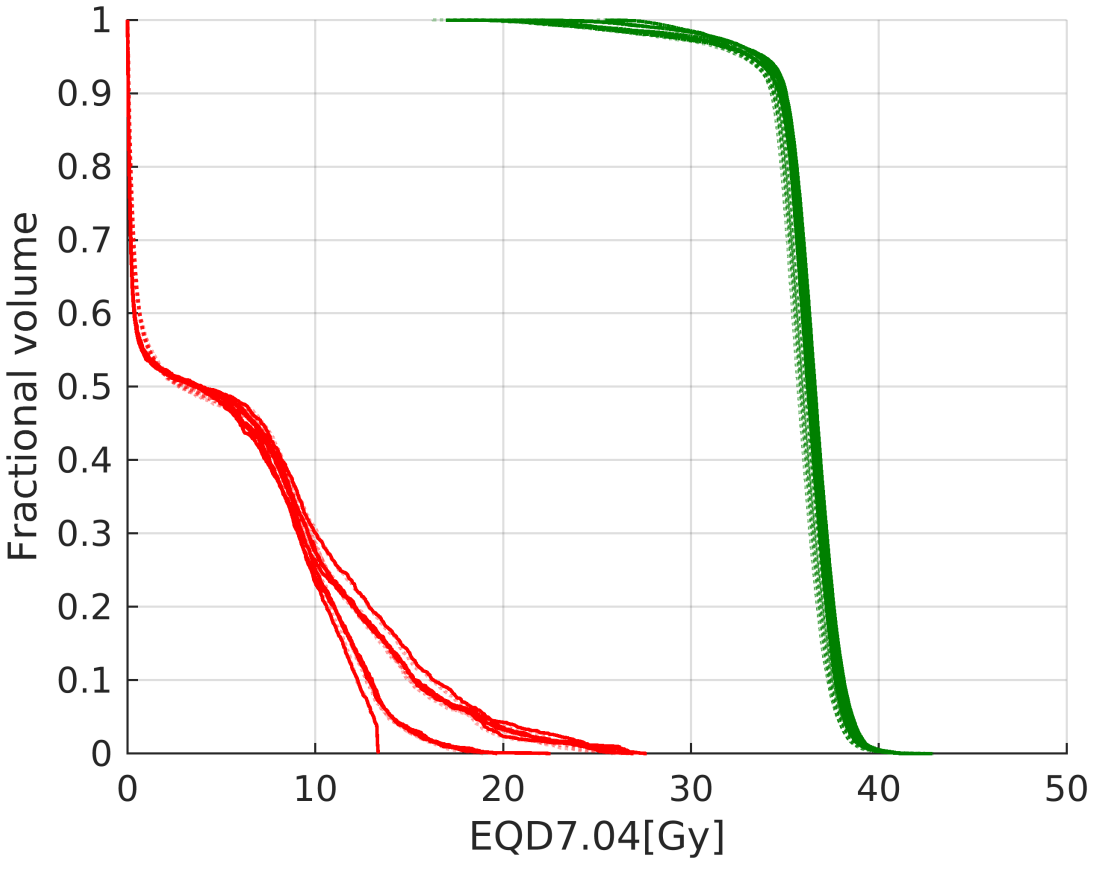
Fractional volume
EQD7.04[Gy]
0
0.1
0.2
0.3
0.4
0.5
0.6
0.7
0.8
0.9
1
0
10
20
30
40
50

(a)

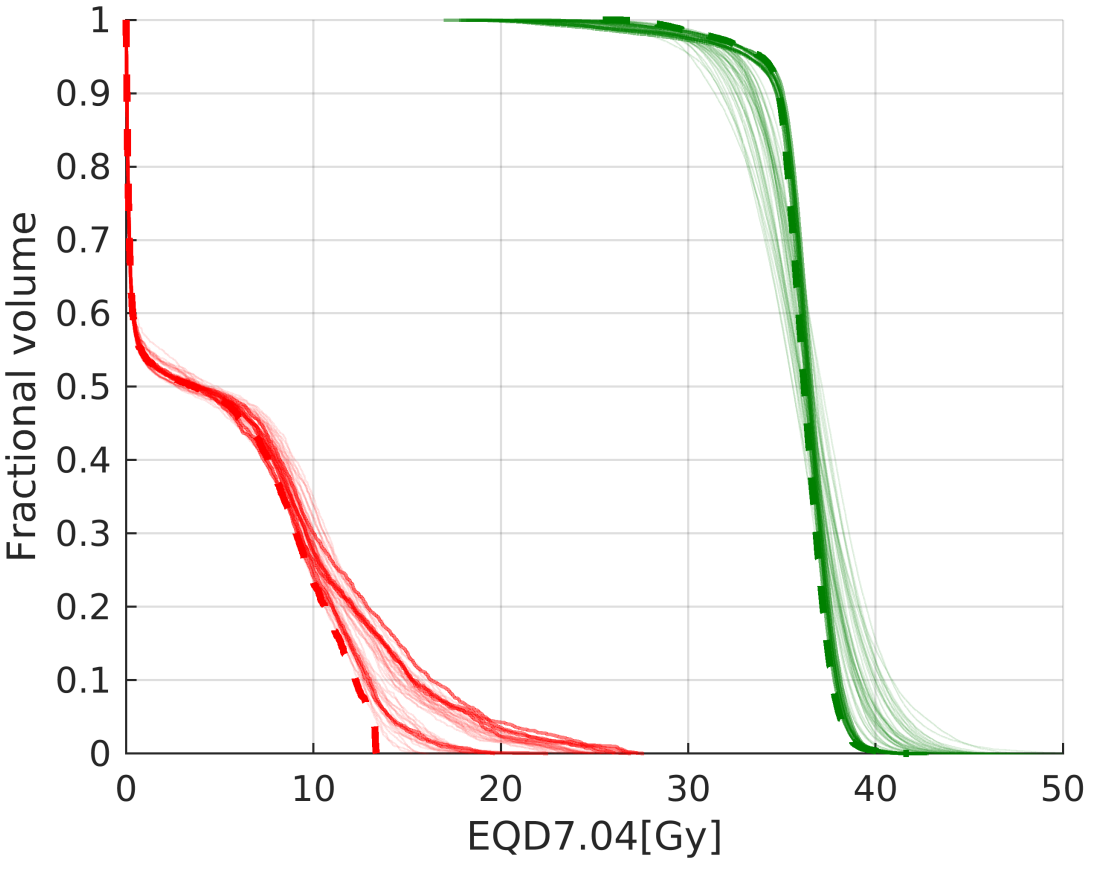
Fractional volume
EQD7.04[Gy]
0
0.1
0.2
0.3
0.4
0.5
0.6
0.7
0.8
0.9
1
0
10
20
30
40
50

(b)

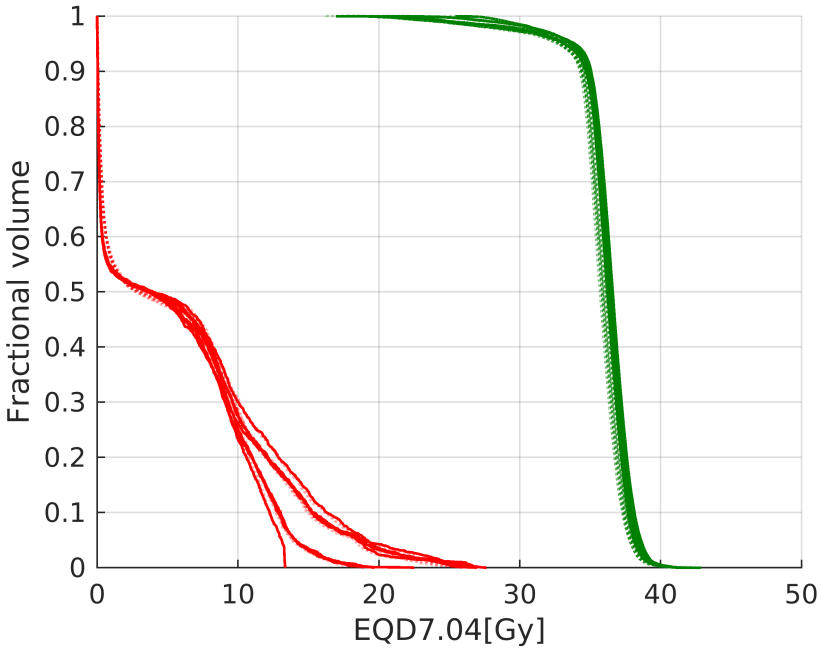
Fractional volume
EQD7.04[Gy]
0
0.1
0.2
0.3
0.4
0.5
0.6
0.7
0.8
0.9
1
0
10
20
30
40
50

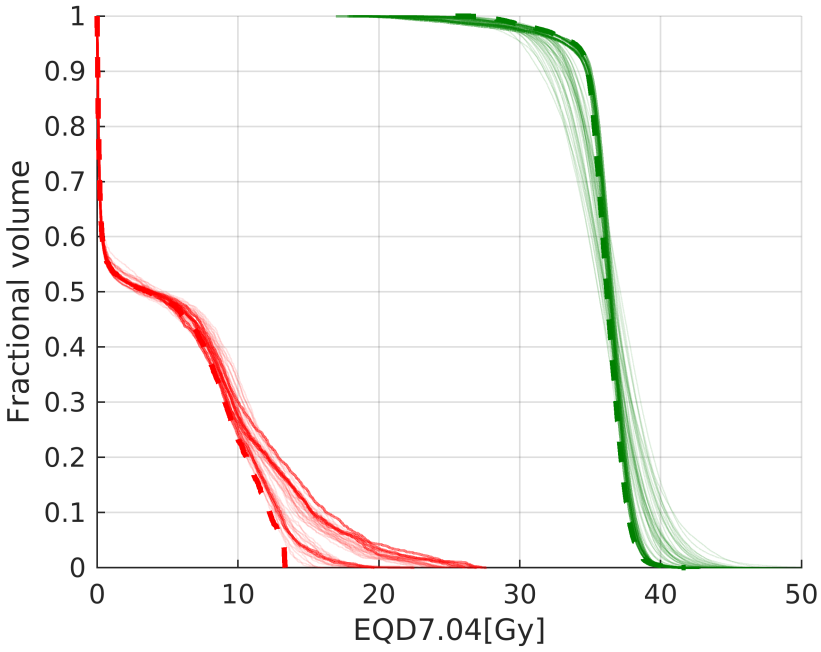
Fractional volume
EQD7.04[Gy]
0
0.1
0.2
0.3
0.4
0.5
0.6
0.7
0.8
0.9
1
0
10
20
30
40
50